

4-1997

Cooperative Power-Limited Optimal Rendezvous Between Many Spacecraft

Virginie Guerre

Embry-Riddle Aeronautical University - Daytona Beach

Follow this and additional works at: <https://commons.erau.edu/db-theses>



Part of the [Aerospace Engineering Commons](#)

Scholarly Commons Citation

Guerre, Virginie, "Cooperative Power-Limited Optimal Rendezvous Between Many Spacecraft" (1997).
Theses - Daytona Beach. 74.

<https://commons.erau.edu/db-theses/74>

This thesis is brought to you for free and open access by Embry-Riddle Aeronautical University – Daytona Beach at ERAU Scholarly Commons. It has been accepted for inclusion in the Theses - Daytona Beach collection by an authorized administrator of ERAU Scholarly Commons. For more information, please contact commons@erau.edu.

COOPERATIVE POWER-LIMITED
OPTIMAL RENDEZVOUS
BETWEEN MANY SPACECRAFT

by
Virginie Guerre

A Thesis Submitted to the
Aerospace Engineering Department
in Partial Fulfillment of the Requirements for the Degree of
Master of Science in Aerospace Engineering

Embry-Riddle Aeronautical University
Daytona Beach, Florida
Avril 1997

UMI Number: EP31823

INFORMATION TO USERS

The quality of this reproduction is dependent upon the quality of the copy submitted. Broken or indistinct print, colored or poor quality illustrations and photographs, print bleed-through, substandard margins, and improper alignment can adversely affect reproduction.

In the unlikely event that the author did not send a complete manuscript and there are missing pages, these will be noted. Also, if unauthorized copyright material had to be removed, a note will indicate the deletion.

UMI[®]

UMI Microform EP31823
Copyright 2011 by ProQuest LLC
All rights reserved. This microform edition is protected against
unauthorized copying under Title 17, United States Code.

ProQuest LLC
789 East Eisenhower Parkway
P.O. Box 1346
Ann Arbor, MI 48106-1346

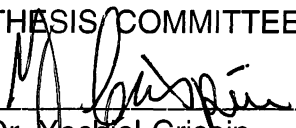
COOPERATIVE POWER-LIMITED OPTIMAL
RENDEZVOUS BETWEEN MANY SPACECRAFT

by

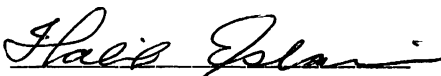
Virginie GUERRE

This thesis was prepared under the direction of the candidate's thesis committee chair, Dr. Yechiel Crispin, Department of Aerospace Engineering, and has been approved by the members of his thesis committee. It was submitted to the Department of Aerospace Engineering and was accepted in partial fulfillment of the requirements for the degree of Master of Science in Aerospace Engineering.


THESIS COMMITTEE:



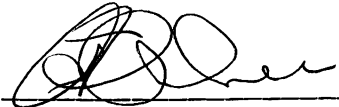
Dr. Yechiel Crispin
Chair



Dr. Habib Eslami
Member



Dr. Seenith Sivasundaram
Member

 5/13/97

Department Chair, Aerospace Engineering

TABLE OF CONTENT

Abstract.....	vi
List of figures.....	vii
Abbreviations.....	xi
Chapters	
1. Introduction.....	1
2. Optimal trajectory equations in a general gravity field.....	13
2.1 Cost function for an optimal trajectory.....	13
2.2 Necessary conditions for an optimum.....	16
2.3 Equation describing an optimal trajectory.....	20
3. Numerical Method.....	9
3.1 The shooting method.....	10
3.2 The finite difference technique for the linear problem.....	11
3.3 The finite difference technique for simple nonlinear problem.....	12
4. Rendezvous of several spacecraft neighboring a circular orbit in the Clohessy-Wiltshire (CW) field.....	22
4.1 Optimal Trajectory equations in the CW field.....	22
4.2 Boundary conditions.....	28
4.3 Transformation to inertial frame.....	31
4.4 The cost.....	34
4.5 Coplanar circular rendezvous.....	35
4.5.1 Trajectories of two spacecraft in a noncooperative rendezvous.....	35

4.5.2 Trajectories of two spacecraft in a cooperative rendezvous.....	37
4.5.3 Trajectories of five spacecraft in a cooperative rendezvous.....	39
4.6 Results.....	40
5. Rendezvous of several spacecraft neighboring an elliptic orbit in the Clohessy-Wiltshire (CW) field.....	41
5.1 Optimal Trajectory Equations in the CW field.....	41
5.2 Boundary conditions.....	46
5.3 Transformation to inertial frame.....	49
5.4 The cost.....	52
5.5 Coplanar elliptic rendezvous: trajectories of two spacecraft in a noncooperative rendezvous.....	53
5.6 Results.....	57
6. Rendezvous of several spacecraft neighboring a circular or elliptic orbit in the Inverse-square gravity field.....	60
6.1 Optimal Trajectory equations in the Inverse-square gravity field.....	60
6.2 Circular and Elliptic orbits.....	62
6.2.a Circular orbit.....	62
6.2.b Elliptic orbit.....	62
6.3 Boundary conditions.....	63
6.3.1 Boundary conditions for a circular orbit.....	64
6.3.2 Boundary conditions for an elliptic orbit.....	65
6.4 The cost.....	66
6.5 Coplanar circular rendezvous.....	67

6.5.1 Trajectories of two spacecraft in a noncooperative rendezvous.....	67
6.5.2 Trajectories of two spacecraft in a cooperative rendezvous.....	69
6.5.3 Trajectories of four spacecraft in a cooperative rendezvous.....	71
6.6 Coplanar elliptic rendezvous: Trajectories of two spacecraft in a noncooperative rendezvous.....	72
6.7 Results.....	75
7. Conclusion.....	77

Appendixes

A. Calculation of the symmetric gravity gradient matrix for the case of a circular orbit.....	79
B. Calculation of the acceleration relative to a rotating observer fixed in the CW frame for a circular orbit.....	83
C. Calculation of the second order primer vector differential equation for a circular orbit.....	86
D. Development of the equation of motion in terms of $\delta \underline{r}$ for circular orbit.....	88
E. Development of the equation of motion in terms of the coordinates x and y for the circular orbit.....	89
F. Calculation of the derivation of n.....	91
G. Calculation of the acceleration relative to a rotating observer fixed in the CW frame for an elliptic orbit.....	92
H. Calculation of the second order primer vector differential equation for an elliptic orbit.....	95
I. Development of the equation of motion in terms of $\delta \underline{r}$ for an elliptic orbit.....	97

J. Calculation of the optimal trajectory equation (6.6) for spacecraft neighboring a circular or elliptic orbit in an Inverse-square gravity field.....	100
References.....	103

ABSTRACT

Author: Virginie Guerre
Title: Cooperative Power-Limited Optimal Rendezvous
Between Many Spacecraft
Institution: Embry-Riddle Aeronautical University
Degree: Master of Science in Aerospace Engineering
Year: 1996

The minimum fuel rendezvous problem between several power-limited low-thrust spacecraft neighboring either a circular or an elliptic orbit is investigated. Both cooperative and non cooperative maneuvers are studied. The maximum principle of Pontryagin is applied to the optimal control rendezvous problem of several spacecraft. The gravitational field models investigated are the Clohessy-Wiltshire field and the inverse-square gravity field. Numerical solutions using a shooting method and the finite difference method are used in order to determine the trajectories of the spacecraft.

Unlike previous investigations, this work is not restricted to a rendezvous of two spacecraft around a circular orbit, but a few vehicles will be able to rendezvous in space at a fixed-final time, both about a circular orbit and about an elliptic orbit.

LIST OF FIGURES

Figure 1. Decomposition of the position vectors.....	23
Figure 2. Rotating frame (X_R, Y_R, Z_R).....	25
Figure 3. Position and Velocity of each spacecraft on the circular orbit in the CW field.....	30
Figure 4. Transformation from the rotating frame to the inertial frame for a circular orbit.....	32
Figure 5. Transformation from the rotating frame to the shifted frame for a circular orbit.....	33
Figure 6. Transformation from the translating frame to the inertial frame for a circular orbit.....	34
Figure 7. Spacecraft Trajectories for a circular noncooperative rendezvous in the CW field : case 1.....	36
Figure 8. Spacecraft Trajectories for a circular noncooperative rendezvous : case 2.....	37
Figure 9. Spacecraft Trajectories for a circular noncooperative rendezvous : case 3.....	37
Figure 10. Spacecraft trajectories for a circular cooperative rendezvous (2 active vehicles) : case 1.....	38
Figure 11. Spacecraft trajectories for a circular cooperative rendezvous (2 active vehicles) : case 2.....	39

Figure 12. Spacecraft trajectories for a circular cooperative rendezvous (2 active vehicles) : case 3.....	39
Figure 13. Spacecraft trajectories for a circular cooperative rendezvous (5 active vehicles).	40
Figure 14. Elliptic orbit.....	42
Figure 15. Position and Velocity of each spacecraft on the elliptic orbit in the CW field.....	47
Figure 16 : Transformation from the rotating frame to the inertial frame for an elliptic orbit.....	50
Figure 17. Transformation from the rotating frame to the shifted frame an elliptic orbit.....	50
Figure 18. Transformation from the shifted frame to the inertial frame for an elliptic orbit.....	51
Figure 19. Spacecraft Trajectories for an elliptic noncooperative rendezvous : case 1.....	53
Figure 20. Spacecraft Trajectories for an elliptic noncooperative rendezvous : case 2 (eccentricity=0.2).....	54
Figure 21. Spacecraft Trajectories for an elliptic noncooperative rendezvous : case 2 (eccentricity=0.42).....	55
Figure 22. Spacecraft Trajectories for an elliptic noncooperative rendezvous : case 3 (eccentricity=0.2).....	56
Figure 23. Spacecraft Trajectories for an elliptic noncooperative rendezvous : case 3 (eccentricity=0.42).....	56
Figure 24. Spacecraft Trajectories for an elliptic noncooperative rendezvous with the finite difference method for linear problems.....	58

Figure 25. Spacecraft Trajectories for an elliptic noncooperative rendezvous with the finite difference method for nonlinear problems.....	59
Figure 26. Circular orbit.....	62
Figure 27. Position and Velocity of each spacecraft on a circular orbit in the Inverse square gravity field.....	64
Figure 28. Position and Velocity of each spacecraft on an elliptical orbit in the Inverse square gravity field.....	65
Figure 29. Spacecraft Trajectories for a circular noncooperative rendezvous : case 1.....	68
Figure 30. Spacecraft Trajectories for a circular noncooperative rendezvous : case 2.....	68
Figure 31. Spacecraft Trajectories for a circular noncooperative rendezvous : case 3.....	69
Figure 32. Spacecraft trajectories for a circular cooperative rendezvous (2 active vehicles) : case 1.....	70
Figure 33. Spacecraft trajectories for a circular cooperative rendezvous (2 active vehicles) : case 2.....	70
Figure 34. Spacecraft trajectories for a circular cooperative rendezvous (2 active vehicles) : case 3.....	71
Figure 35. Spacecraft trajectories for a circular cooperative rendezvous (4 active vehicles).....	71
Figure 36. Spacecraft Trajectories for an elliptic noncooperative rendezvous : case 1.....	72
Figure 37. Spacecraft Trajectories for an elliptic noncooperative rendezvous : case 2 ($T=3\pi / 4$).....	73

Figure 38. Spacecraft Trajectories for an elliptic noncooperative rendezvous :	
case 2 ($T=\Pi$).....	73
Figure 39. Spacecraft Trajectories for an elliptic noncooperative rendezvous :	
case 3 (eccentricity=0.2).....	74
Figure 40. Spacecraft Trajectories for an elliptic noncooperative rendezvous :	
case 3 (eccentricity=0.5).....	75
Figure 41. Spacecraft Trajectories for a circular noncooperative rendezvous	
with the finite difference method for nonlinear problems.....	76

ABREVIATIONS

CW : Clohessy-Wiltshire

BC : Boundary Conditions

CHAPTER 1

Introduction

Historically, spacecraft rendezvous studies involved one thrusting (active) vehicle and one coasting (passive) vehicle, also called noncooperative rendezvous. The term “cooperative” indicates that each vehicle is active, which means capable of providing part or all of the total velocity change necessary to obtain a rendezvous. Optimal rendezvous implies that the sum of the final masses of the vehicles is maximized or in other words, that the total propellant consumption is minimized. A comparison of the costs of cooperative rendezvous would be meaningful if all the vehicles have comparable size and the same propulsion system. In our research, they are all power-limited. It was shown that the cooperative rendezvous presents an important advantage : a reduction in total propellant is obtained as compared to the traditional active-passive rendezvous when the vehicles are all active [Coverstone, 1992, 1993, 1994].

The problem of finding optimal spacecraft trajectories has received considerable attention over the last few decades. Several scientists have studied different aspects of optimal rendezvous using optimal control theory. Studying the cooperative rendezvous, Prussing and Conway [Prussing, 1989] determined the optimal terminal maneuver for a cooperative impulsive rendezvous. They found how much of the total required velocity change should be provided by each vehicle for two active spacecraft. [Mirfakhraie, 1991] and Mirfakhraie and

Conway [Mirfakhraie, 1990] developed a method for determining optimal minimum-fuel trajectories for the fixed-time cooperative rendezvous of two spacecraft with impulsive propulsion systems. They concluded that a cooperative type of rendezvous is advantageous when the time allowed for rendezvous is relatively short. Coverstone [Coverstone, 1992, 1993] considered the optimal cooperative power-limited rendezvous between two spacecraft neighboring a circular orbit. In that problem the motion is not restricted to the plane, the z-component is taken in account. Recently, Coverstone-Carroll and Prussing [Coverstone, 1994] studied the optimal cooperative power-limited rendezvous between circular coplanar orbits for the inverse-square gravity field and the Clohessy-Wiltshire field. They concluded that the total propellant used for both cooperative and noncooperative rendezvous decreases as total maneuver time increases and that the cooperative rendezvous uses less total propellant than the corresponding active-passive rendezvous. They noticed also that the addition of circular terminal orbit constraints increases total propellant consumption when compared to the unconstrained cooperative rendezvous. The word "constraint" means that the circular terminal orbit is specified and is always between the two initial orbit radii. However, on the contrary, the word "unconstrained" means that the final position is not constrained to occur on a given circular trajectory. The final position is not specified. Only the ellipse time for the rendezvous is specified. Carter [Carter, 1994] studied the optimal power-limited rendezvous for linearized equations of motion. The solution is then applied to the problem of rendezvous of a spacecraft with an object in the vicinity of a nominal Keplerian orbit. He concluded that for rendezvous with satellites in elliptical, parabolic, or hyperbolic orbits, the optimal solution is given almost in closed form. For rendezvous with satellites in near-circular orbits, Carter linearized the problem about a nominal orbit that is circular and solved it in closed- form.

Carter treated the same problem as the one of Coverstone and Prussing described above but the mathematical approach and the method of solution were different. Carter and Brient [Carter, 1992] contributed to the related linear bounded-thrust rendezvous near an arbitrary Keplerian orbit in fixed time. Bounded-thrust fuel optimal spacecraft trajectories are compared for elliptical, parabolic and hyperbolic orbits. They developed a transformation from the original state vector to a new pseudostate vector. The advantage of this transformation is that the new pseudostate vector is constant unless the spacecraft thrusters are activated. This approach avoids the problem of inverting a fundamental matrix solution.

In general spacecraft trajectories are classified into two types : high-thrust and low-thrust. The high-thrust programs are distinguished from the low-thrust programs by examining the ratio of thrust acceleration to gravitational acceleration. For high-thrust, this ratio is much greater than one and the thrust time is relatively short compared to the time between thrusting. For this reason, the high -thrust is also called impulsive thrust. For low-thrust, the ratio is on the order of less than one tenth and the thrust level results in prolonged thrusting intervals. Dual-thrust programs are also possible. It has been shown that when the individual performances are the same, a dual-thrust program is more effective than individual high and low-thrust programs [Larson, 1989] [Lembeck, 1993].

Propulsion systems can be further categorized as constant specific impulse (CSI) or variable specific impulse (VSI). CSI engines, also called constant exhaust velocity engines, modify their thrust levels by varying the mass flow rate. They can be either high or low thrust devices. Low-thrust CSI engines are “thrust-limited”. The thrust produced by these engines is limited by a maximum value

attainable by the mass flow rate. VSI engines are low-thrust engines. However, the thrust is controlled by varying the exhaust velocity. The power available from a separate energy source required to run the engine is limited. This kind of engine is then referred to as “power-limited” engine. Many papers describe low-thrust spacecraft maneuvering. Prussing [Prussing, 1993 (a)][Prussing, 1993 (b)] obtained the general equations for optimal power-limited spacecraft trajectories. The equations of motion and the necessary conditions for an optimal trajectory have been combined into a single fourth order differential equation for the position vector. Murphy [Murphy, 1992] studied the optimal power-limited spacecraft rendezvous trajectories for different gravity fields : free field, constant gravity field and linearized gravity field. He could not find any solution for the inverse square-gravity field because of a lack of convergence in one of his routines. Pardis and Carter [Pardis, 1995] considered the effect of an upper bound on the thrust magnitude (thrust saturation) in the linearized power-limited rendezvous problem. In addition to a limit on the power, there is a limit on the thrust. They presented a necessary condition for a solution of the problem in terms of the bound on thrust and the boundary conditions. They also found a necessary and sufficient condition for an optimal solution to be fuel efficient in terms of the bound on the thrust and the boundary conditions. They concluded that the smaller the region of saturation the better; the best situation being a totally unsaturated flight.

Other works described high-thrust spacecraft rendezvous or high and low-thrust spacecraft rendezvous. For example, Chiu and Prussing [Prussing, 1986] [Chiu, 1984] studied the optimal multiple impulse time-fixed rendezvous between circular orbits. The coplanar case and a restricted class of noncoplanar cases were analysed. In the linearized case, as many as four impulses are required for an optimal fixed time rendezvous. In the noncoplanar linearized case, the

maximum number of impulses required is six. Prussing and Clifton [Prussing, 1994] determined the minimum-fuel, impulsive solutions obtained for the evasive maneuver of a satellite followed by a rendezvous with the original orbit station for both final-time constrained and final-open maneuvers. The returns-on-station maneuvers considered are likely the most expensive in terms of fuel compared to other maneuvers. Larson-Lembeck and Prussing [Larson, 1989], [Lembeck, 1993] worked on an optimal orbital rendezvous using high and low thrust. The high-thrust program is used first in order to perform an intercept of a predetermined position in space in a specified amount of time. Then, the spacecraft returns to the original orbit station with a low-thrust propulsion system using optimal control. Dual thrust programs seem more effective than individual high and low-thrust programs.

In this thesis, the power-limited rendezvous problem is considered. The optimal power-limited spacecraft is one which will have many applications as new power-limited engines are developed. Since the engines are low-thrust, they will be useful in orbit transfers between neighboring orbits, or in deep space orbit transfers, when the engine are operated continuously in order to build up the acceleration needed. In the first part of this study, we will work on spacecraft neighboring circular orbits and in the second and last part, we will consider spacecraft neighboring elliptic orbits. Rao and Romanan [Rao, 1992] treated the case of optimal rendezvous transfer between coplanar heliocentric elliptic orbits using solar sail. They pointed out the effect of the eccentricities of the terminal orbits on the time-optimal transfer. The optimal control problem studied is converted to a two-point boundary-value problem consisting of a system of seven first-order ordinary differential equations. Tschauner [Tschauner, 1967] worked on the rendezvous between a spacecraft propelled by engines with

restricted thrust and an unpropelled target moving in an elliptic orbit of arbitrary eccentricity. Euler [Euler, 1969] studied the coplanar rendezvous maneuver between a thrusting vehicle and a passive vehicle in an elliptic orbit. His work was limited to a terminal phase of an interception. He calculated an analytic solution for the fuel optimal thrust program for power-limited vehicles when the time to maneuver is fixed. He realised that the solution to the homogeneous linear equations of motion for elliptic target orbits permits the reduction of the low-thrust rendezvous optimal control problem to quadrature. Wellnitz and Prussing [Wellnitz, 1987] studied the optimal trajectories for time-constrained rendezvous between arbitrary conic orbits. Primer vector theory is used to determine how the cost can be minimized by the addition of initial and final coast periods, and by the addition of midcourse impulses.

Analytical methods, such as the state transition matrix method, for solving optimal spacecraft trajectories were used in the past. This kind of problem can not be solved analytically when more than two vehicles are involved since it becomes too complicated and intractable. For the elliptic orbit problem, an analytic solution is also very difficult to obtain because the coefficients of the differential equations are time-dependent. In this thesis, numerical solutions are used for solving both the circular and the elliptic cases with more than two vehicles in two different fields : the CW and the inverse square gravity field. Humi [Humi, 1993] studied the fuel optimal rendezvous in a general central force field. Only the formulation of the equations of motion and the optimal control for the linearized equations of motion were presented. No specific result have been obtained.

In order to obtain minimum-fuel solutions, we apply optimal control theory. The optimal controller is determined by using the Pontryagin Minimum Principle

[Bryson, 1969]. For convenience, we will use the primer vector described by Lawden [Lawden, 1963], [Coverstone, 1992]. Lawden introduced for the first time the primer vectors in an optimal control problem in 1963 in the course of his pioneering work on minimum-fuel orbital transfers. Lawden used the term “primer vector” to describe the adjoint to the velocity vector because of its significance for the optimal trajectory.

Two approaches are considered in order to solve optimal control problems. The “indirect” approach uses the calculus of variations to derive the necessary conditions of optimality, i.e., the Euler-Lagrange equations. This results in a two point boundary-value problem (TPBVP), which may then be solved numerically. On the other hand, the “direct” approach uses mathematical programming. It consists of transforming the original problem into a parameter optimization problem. Explicit integration of the system of differential equations is avoided. Instead, algebraic expressions (Hermite cubic polynomials) approximate the differential equations locally, and the resulting system of nonlinear simultaneous equations is then solved by mathematical programming. A well-known indirect approach for solving the optimal control problem that results in a TPBVP is the “shooting” method. This method requires a first guess of either the initial or final boundary conditions. In order to find the conditions at the other end, the Euler-Lagrange system is then integrated forward or backward. Adjusting the guess and iterating the process, the appropriate conditions that satisfy the problem will eventually be found. Colasurdo and Pastrone [Colasurdo, 1993] presented an indirect technique that optimizes fixed-time finite-thrust orbit transfers. The technique used, which is fairly general and extendible to a wide variety of problems, seemed to reduce the sensitivity of the indirect methods to the initial value of the adjoint variables. The procedure appeared to be very accurate. Hargraves and Paris [Hargraves, 1987] described the direct trajectory

optimization using nonlinear programming and collocation. The method employs cubic polynomials to represent state variables, linearly interpolates control variables, and uses collocation to satisfy the differential equations. The method is easy to program for a general trajectory optimization problem. They used an implicit integration scheme based on Hermite interpolation to convert the optimal control problem to a nonlinear programming problem. Scheel and Conway [Scheel, 1994] determined optimum very low-thrust transfer using a direct transcription approach to convert the continuous optimal control problem into a nonlinear programming problem. Many-revolution spacecraft trajectories are considered. They added a parallel Runge-Kutta shooting algorithm in order to decrease the size of the nonlinear programming problem resulting from the direct transcription process. They demonstrated that Runge-Kutta parallel shooting transcription and nonlinear programming method can be successfully applied to the optimization of many-revolution orbit raising trajectories about Earth. Also, Tang and Conway [Tang, 1995] demonstrated the success of the method of direct collocation with nonlinear programming applied to the problem of optimization of very low thrust interplanetary transfers.

The method used in this thesis are the shooting method and the finite difference method [Zwillinger, 1989]. For the implementation, we use the Matlab software package. Matlab is a technical computing environment for high-performance numeric computation and visualization. The advantage of Matlab is its easy access to work on matrices and algebra in general.

CHAPTER 2

Optimal trajectory equations in a general gravity field.

In this chapter, the equations of motion for a rendezvous of power limited vehicles in a general gravitational field will be developed. The cost functional and the Hamiltonian will be calculated in order to find the optimal solution of the problem. The general equations found in this chapter will be useful for the following chapters. In the next chapters, we will study the problem of several spacecraft in a cooperative or noncooperative rendezvous for a fixed gravity field, and in the vicinity of a circular or elliptic orbit using the optimal equations. Although, many spacecraft are considered, the gravitational forces between the spacecraft are neglected. Only the gravitational forces between each spacecraft and the planet are taken into account.

2.1 Cost function for an optimal trajectory

The equations of motion in an inertial frame of reference of a vehicle in terms of a general gravitational field [Prussing, 1993 (a),(b)] are :

$$(2.1) \quad \begin{aligned} \dot{\mathbf{r}} &= \mathbf{v} \\ \dot{\mathbf{v}} &= \mathbf{g}(\mathbf{r}) + \mathbf{\Gamma} \\ \dot{m} &= -b \leq 0 \end{aligned}$$

Where \underline{r} and \underline{v} are the position and absolute velocity vectors of the spacecraft, g is the gravitational acceleration and $\underline{\Gamma}$ is the thrust acceleration of the engine.

The mass is denoted by m and b is the mass flow rate of the engine.

The thrust acceleration magnitude is :

$$(2.2) \quad \Gamma = \frac{T}{m}$$

The exhaust power of a power limited engine is related to the thrust [Murphy, 1992] by the following equation :

$$(2.3) \quad P = \frac{1}{2} Tc$$

Where P is the exhaust power, T the thrust and c the velocity of the exhaust particles. The thrust T may be written in terms of the mass flow rate b as follows [Murphy, 1992]:

$$(2.4) \quad T = bc \quad \text{with} \quad b = -\dot{m} \geq 0$$

where c is the exhaust velocity.

The thrust acceleration Γ is then given by :

$$(2.5) \quad \Gamma = \frac{bc}{m}$$

Optimizing the fuel cost is equivalent to minimizing the mass of the propellant used, or in other words to maximize the final mass. The change in mass is expressed as :

$$(2.6) \quad \frac{d}{dt} \left(\frac{1}{m} \right) = \frac{-\dot{m}}{m^2} = \frac{b}{m^2}$$

Using (2.3) and (2.4), we find :

$$(2.7) \quad b = \frac{2P}{c^2}$$

and using (2.3) and (2.5), we get :

$$(2.8) \quad m = \frac{2P}{\Gamma c}$$

Using (2.7) and (2.8), the change of mass is :

$$(2.9) \quad \frac{d}{dt} \left(\frac{1}{m} \right) = \frac{b}{m^2} = \frac{2P}{c^2} \times \frac{\Gamma^2 c^2}{(2P)^2} = \frac{\Gamma^2}{2P}$$

Integrating the equation (2.9) to find the change in mass between the initial and final times :

$$(2.10) \quad \frac{1}{m_f} - \frac{1}{m_0} = \frac{1}{2} \int_{t_0}^{t_f} \frac{\Gamma^2(t)}{P(t)} dt$$

Here m_0 is the initial mass of the vehicle, the final mass m_f is maximized by minimizing $\frac{1}{m_f}$.

$$(2.11) \quad \frac{1}{m_f} = \frac{1}{m_0} + \frac{1}{2} \int_{t_0}^{t_f} \frac{\Gamma^2(t)}{P(t)} dt$$

The limited power available from a separate power source is usually prescribed as an upper bound [Prussing, 1993 (a), (b)] :

$$(2.12) \quad P \leq P_{\max}$$

The solution to the equation of motion depends only on the initial conditions $\underline{r}(t_0)$ and $\underline{v}(t_0)$ and the vector $\underline{\Gamma}(t)$. Therefore, to minimize the integral term in equation (2.11), we choose to set the power to a constant value, its maximum value,

$$(2.13) \quad P \equiv P_{\max}.$$

Therefore :

$$(2.14) \quad \frac{1}{m_f} = \frac{1}{m_0} + \frac{1}{2} \frac{1}{P_{\max}} \int_{t_0}^f \Gamma^2(t) dt$$

So, from the previous equation, the cost functional to be minimized can be taken to be simply [Prussing, 1993 (a), (b)], [Murphy, 1992] :

$$(2.15) \quad J = \frac{1}{2} \int_{t_0}^f \Gamma^2(t) dt$$

2.2 Necessary conditions for an optimum

To apply the necessary conditions for a minimum of cost functional J, we use the Hamiltonian function [Murphy, 1992]:

$$(2.16) \quad H = L + \underline{\lambda}^T \underline{f}$$

where L is the integrand of the cost functional [Murphy, 1992].

$$(2.17) \quad L = \frac{1}{2} \Gamma^2$$

The vector $\underline{\lambda}(t)$ is a vector of Lagrange multiplier functions (also called adjoint variables) and \underline{f} is the right hand side of the equations of motion (2.1).

The adjoint vector can be partitioned into components that will complement the state vector [Murphy, 1992] :

$$(2.18) \quad \underline{\lambda} = \begin{bmatrix} \underline{\lambda}_r \\ \underline{\lambda}_v \end{bmatrix}$$

The state vector was defined as follows :

$$(2.19) \quad \underline{x} = \begin{bmatrix} \underline{r} \\ \underline{v} \end{bmatrix}$$

The vector \underline{r} is the position vector and the vector \underline{v} is the velocity vector (derivative of \underline{r}). Let's write the thrust acceleration vector is :

$$(2.20) \quad \underline{\Gamma} = \Gamma \underline{u}$$

where \underline{u} is the directional unit vector for the thrust.

According to the equation of motion (2.1) above :

$$\underline{\dot{v}} = g(\underline{r}) + \Gamma \underline{u}$$

we can write this equation as a first order system :

$$(2.21) \quad \underline{\dot{x}} = f(x, \Gamma, u, t)$$

$$\underline{\dot{x}} = \begin{bmatrix} \underline{\dot{r}} \\ \underline{\dot{v}} \end{bmatrix} = \begin{bmatrix} \underline{v} \\ g(\underline{r}) + \Gamma \underline{u} \end{bmatrix}$$

Using equations (2.17) and (2.18) in the Hamiltonian function (2.16), we get :

$$(2.22) \quad H = \frac{1}{2} \Gamma^2 + \underline{\lambda}_r^T \cdot \underline{v} + \underline{\lambda}_v^T (g(\underline{r}) + \Gamma \underline{u})$$

The necessary condition for the adjoint vector is of the general form [Bryson, 1969] :

$$(2.23) \quad \dot{\underline{\lambda}}^T = -\frac{\partial H}{\partial \underline{x}}$$

Applying this equation to the Hamiltonian function found in (2.22), we get :

$$(2.24) \quad \dot{\underline{\lambda}}_r^T = -\frac{\partial H}{\partial \underline{r}} = -\underline{\lambda}_v^T G(\underline{r})$$

$$(2.25) \quad \dot{\underline{\lambda}}_v^T = -\frac{\partial H}{\partial \underline{v}} = -\underline{\lambda}_r^T$$

where G is the gravity gradient matrix $\frac{\partial g}{\partial \underline{r}}$.

The optimal controller is determined by using the Pontryagin Minimum Principle [Bryson, 1969]. This theory leads us to choose Γ and \underline{u} so that they minimize the Hamiltonian H. The value of the Hamiltonian is minimized with respect to the thrust direction \underline{u} by aligning \underline{u} opposite to the adjoint vector $\underline{\lambda}_v$ [Prussing, 1993 (a), (b)].

$$(2.26) \quad \underline{u} = -\frac{\underline{\lambda}_v}{\lambda_v}$$

Introducing the primer vector \underline{p} after Lawden [Lawden, 1963] :

$$(2.27) \quad \underline{p}(t) = -\underline{\lambda}_v(t)$$

\underline{u} can be written as :

$$(2.28) \quad \underline{u} = \frac{\underline{p}}{p}$$

The necessary condition on the adjoint vector given in (2.24) and (2.25) leads to the equations :

$$(2.29) \quad \dot{\underline{p}} = \underline{\lambda}_r$$

$$(2.30) \quad \ddot{\underline{p}} = G(\underline{r})\underline{p}$$

Using the equations (2.27), (2.28) and (2.29) in (2.22), the Hamiltonian can be expressed in the form :

$$(2.31) \quad H = \frac{1}{2}\Gamma^2 + \underline{\dot{p}}^T \underline{v} - \underline{p}^T \underline{g} - \Gamma p$$

According to the minimum principle of Pontryagin, the Hamiltonian equation (2.31) is minimized with respect to the thrust acceleration magnitude Γ by setting

$$(2.32) \quad \frac{\partial H}{\partial \Gamma} = \Gamma - p = 0$$

which yields :

$$(2.33) \quad \Gamma = p$$

The second partial derivative of H with respect to Γ is determined to ensure that we are in the case of a minimum.

$$\frac{\partial^2 H}{\partial \Gamma^2} = 1 > 0 \text{ proves that the H minimum is achieved.}$$

Using the equations (2.28) and (2.33), we find :

$$(2.34) \quad \underline{\Gamma} = \Gamma \frac{\underline{p}}{p} = p \frac{\underline{p}}{p} = \underline{p}$$

The optimal thrust acceleration vector $\underline{\Gamma}$ is equal to the primer vector \underline{p} governed by the equations (2.27), (2.29) and (2.30).

In conclusion, the equations that will be used to find an optimal trajectory equation for a power limited spacecraft that only involves functions and derivatives of the position vector \underline{r} are equations (2.30) and (2.34) given above :

$$\begin{aligned} \underline{\Gamma} &= \underline{p} \\ \underline{\ddot{p}} &= G(\underline{r})\underline{p} \end{aligned}$$

2.3 Equation describing an optimal trajectory

Combining the two first equations of (2.1), we find :

$$(2.35) \quad \ddot{\underline{r}} = \underline{g}(\underline{r}) + \underline{\Gamma}$$

From equation (2.20) :

$$\underline{\Gamma} = \underline{\Gamma} \underline{u}$$

Differentiating equation (2.35) twice with respect to time, we obtain :

$$(2.36) \quad \underline{r}^{IV} = \ddot{\underline{g}}(\underline{r}) + \ddot{\underline{\Gamma}}$$

According to equation (2.30) :

$$\ddot{\underline{p}} = G(\underline{r}) \underline{p}$$

and to equation (2.34) :

$$\underline{\Gamma} = \underline{p}$$

the primer vector \underline{p} can be expressed as the following using equation (2.35) :

$$(2.37) \quad \underline{p} = \underline{\Gamma} = \underline{\Gamma} \underline{u} = \ddot{\underline{r}} - \underline{g}(\underline{r})$$

Therefore from (2.30), $\ddot{\underline{\Gamma}}$ can be written :

$$(2.38) \quad \ddot{\underline{\Gamma}} = G(\underline{r}) \underline{p}$$

Combining equations (2.38) and (2.37) :

$$(2.39) \quad \ddot{\underline{\Gamma}} = G(\underline{r})(\ddot{\underline{r}} - \underline{g}(\underline{r}))$$

Substituting equation (2.39) into equation (2.36), we obtain :

$$(2.40) \quad \underline{r}^{IV} = \ddot{\underline{g}}(\underline{r}) + G(\underline{r})(\ddot{\underline{r}} - \underline{g}(\underline{r}))$$

To find $\ddot{\underline{g}}$, we first evaluate $\dot{\underline{g}}$:

$$(2.41) \quad \dot{\underline{g}}(\underline{r}) = \frac{d(\underline{g}(\underline{r}))}{dt} = \frac{\partial \underline{g}}{\partial \underline{r}} \frac{\partial \underline{r}}{\partial t} = G(\underline{r}) \cdot \dot{\underline{r}}(t)$$

Differentiating once with respect to time, we obtain :

$$(2.42) \quad \ddot{\underline{g}}(\underline{r}) = \dot{G}(\underline{r}) \dot{\underline{r}}(t) + G(\underline{r}) \ddot{\underline{r}}(t)$$

Substituting (2.42) into (2.40), we get the optimal trajectory equation :

$$(2.43) \quad \underline{r}^{IV} = \dot{G}(\underline{r}) \dot{\underline{r}}(t) + G(\underline{r}) \ddot{\underline{r}}(t) + G(\underline{r})(\ddot{\underline{r}}(t) - \underline{g}(\underline{r}))$$

Grouping the terms together and simplifying , we get :

$$(2.44) \quad \underline{r}^{IV} = \dot{G}(\underline{r})\dot{\underline{r}}(t) + 2G(\underline{r})\ddot{\underline{r}}(t) - G(\underline{r})g(\underline{r})$$

The equation (2.44) is the optimal (mimumum fuel) trajectory equation in an inertial frame of reference for a power-limited spacecraft given in terms of functions and derivatives of the position \underline{r} .

The boundary conditions on a rendezvous trajectory are given as a known initial vector $\underline{r}(t_0)$ and a known initial velocity vector $\underline{v}(t_0)$, along with final constraints of the form :

$$(2.45) \quad \psi(\underline{r}(t_f), \underline{v}(t_f), T) = 0$$

CHAPTER 3

Numerical Methods

In order to solve the Boundary Value Problems that occur in the cases of spacecraft neighboring circular or elliptic orbits in two different gravity fields, we choose different numerical methods. The most popular one, the shooting method [Zwillinger, 1989] is one of them. This method consists of guessing the missing Boundary conditions and integrates the differential equations until the numerical approximations found are very close of the exact values. The Newton's method will be used to determine how close the approximations are of these exact values. This method is used for all of the rendezvous problems of this thesis.

The other method is the finite difference technique. Matlab, the Software used for solving the rendezvous problem, has already predefined functions that are very useful for the type of problems considered. One of these functions solves the boundary value problem with a finite difference technique for a general linear problem. This problem is particularly well adapted to the case of the CW field for either a circular and an elliptic orbits because the differential equations found are linear. The other function of Matlab solves the boundary value problem with a finite difference technique for simple nonlinear problem. That's the case of the inverse-square gravity field for either a circular or an elliptic orbit. The finite difference technique for nonlinear problems will also be used for linear problems of the CW field type.

Let's see in more details all of these three methods.

The general procedure will be illustrated with general equations close to the one of the problems treated in order to understand the technique. We have two coupled differential equations of fourth order. We wish to numerically approximate the solution of these equations.

$$(3.1) \quad \begin{aligned} x^{(4)} + a_1 y^{(3)} + b_1 x^{(2)} + c_1 \dot{y} + d_1 x &= 0 \\ y^{(4)} + a_2 x^{(3)} + b_2 y^{(2)} + c_2 \dot{x} + d_2 y &= 0 \end{aligned}$$

with initial conditions :

$$(3.2) \quad \begin{aligned} x(t_o) &= A & y(t_o) &= C \\ \dot{x}(t_o) &= B & \dot{y}(t_o) &= D \end{aligned}$$

and final conditions :

$$(3.3) \quad \begin{aligned} x(t_f) &= E & y(t_f) &= G \\ x'(t_f) &= F & \dot{y}(t_f) &= H \end{aligned}$$

where A, B, C, D are given constants for the initial conditions and E, F, G, H are given constant for the final conditions. It is important to note that the differential equations (3.1) can be either linear or nonlinear equations.

3.1 The shooting method

The method consists of taking a intermediary variables called z such that :

$$(3.4) \quad \begin{aligned} z_1 &= x & & & z_5 &= y \\ z_2 &= \dot{x} & \text{and} & & z_6 &= \dot{y} \\ z_3 &= \ddot{x} & & & z_7 &= \ddot{y} \\ z_4 &= \dddot{x} & & & z_8 &= \dddot{y} \end{aligned}$$

So the differential equations (3.1) will be a system of eight single differential equations of the form :

$$\begin{aligned}
 \dot{z}_1 &= z_2 \\
 \dot{z}_2 &= z_3 \\
 \dot{z}_3 &= z_4 \\
 (3.5) \quad \dot{z}_4 &= -a_1 z_8 - b_1 z_3 - c_1 z_8 - d_1 z_1 \\
 \dot{z}_5 &= z_6 \\
 \dot{z}_6 &= z_7 \\
 \dot{z}_7 &= z_8 \\
 \dot{z}_8 &= -a_2 z_4 - b_2 z_7 - c_2 z_2 - d_2 z_5
 \end{aligned}$$

The procedure is to integrate the system of differential equations (3.5) numerically for some arbitrary initial guesses for the missing initial boundary conditions and to compare the final conditions obtained with the required final conditions in (3.3). We will repeat this process until the final conditions found with the differential equations are close enough of the final conditions fixed by the problem. Predefined functions of Matlab are used to integrate the system of differential equations knowing the initial conditions ('ODE45 ') as well as a Newton's method function that evaluate how close the approximation are with respect to the exact values ('fsolve').

3.2 The finite difference technique for the linear problem

We still have the two same coupled differential equations (3.1) that we can write in the form :

$$(3.6) \quad y' = F(x)y + g(x) \quad \text{on the range } [a, b]$$

and the boundary conditions are expressed in the form :

$$(3.7) \quad Cy(a) + Dy(b) = \gamma$$

$F(x)$, C and D are matrices and $g(x)$ and γ are vectors.

Once the differential equations (3.1) are written in the form (3.6) and the boundary conditions in the form (3.7), the predefined function called 'DO2GBF' is used to solve the problem. This function is part of the NAG (Numerical Algorithms Group Ltd) Toolbox for used with Matlab.

3.3 The finite difference technique for simple nonlinear problem

The system of differential equations (3.1) is written in the form :

$$(3.8) \quad \dot{y}_i = f_i(x, y) \quad i=1,2, \dots, n \quad \text{on the range } [a, b]$$

with part of the boundary conditions given at $x=a$ and the other boundary conditions at $x=b$.

Once the differential equations of (3.1) are in the form (3.8), the predefined function of Matlab called 'DO2GAF' is used. This routine uses a Newton iteration technique and computes the solution on a mesh of points.

CHAPTER 4

Rendezvous of several spacecraft neighboring a circular orbit in the Clohessy-Wiltshire (CW) field .

The first case investigated using the optimal control theory is the Clohessy-Wiltshire gravity field (CW). When the motion of the spacecraft remains in the vicinity of a circular orbit at all times, the gravity field can be simplified as will be below. This is known as the Clohessy-Wiltshire gravity field. We assume in this chapter, that the vehicles neighbor a circular orbit. The case of an elliptic orbit will be studied in chapter 5. We will work on the equations of motion and the trajectories of the two or more spacecraft for a cooperative and non cooperative rendezvous. Different examples based on the number of active spacecraft and the location of the spacecraft on the circular orbit will be studied using the numerical methods developed in chapter 3.

4.1 Optimal Trajectory equations in the CW field

In chapter 2, the equation of motion in the inertial frame was found as :

$$(2.35) \quad \ddot{\underline{r}} = \underline{g}(\underline{r}) + \underline{\Gamma}$$

We assume the motion of the spacecraft remains in the vicinity of a reference circular orbit at all times, see figure 1.

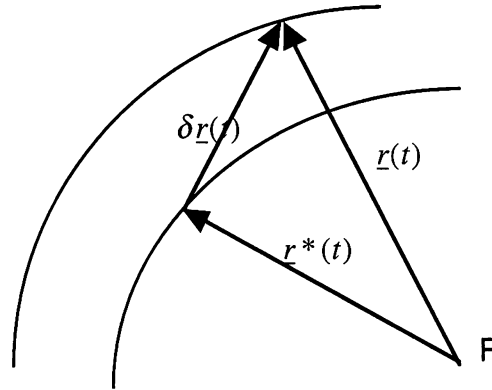


Figure 1 : Decomposition of the position vectors

The vector difference between the vehicle position and the reference position is known as the relative position vector $\delta \underline{r}(t)$ [Prussing, 1993 (c)] :

$$(4.1) \quad \delta \underline{r}(t) = \underline{r}(t) - \underline{r}^*(t)$$

where $\underline{r}(t)$ represents the orbit of the vehicle, and $\underline{r}^*(t)$ represents the orbit of a reference body in a reference orbit.

The problem is to find a simple, approximate equation describing $\delta \underline{r}(t)$ and according to equation (4.1), the solution to this simple equation can then be added to the known vector $\underline{r}^*(t)$ to determine $\underline{r}(t)$.

Substituting (4.1) into equation (3.1) yields :

$$(4.2) \quad \ddot{\underline{r}} = \ddot{\underline{r}}^* + \delta \ddot{\underline{r}} = \underline{g}(\underline{r}^* + \delta \underline{r}) + \underline{\Gamma}$$

Using the Taylor series to expand the vector \underline{g} about the reference orbit $\underline{r}^*(t)$, we obtain :

$$(4.3) \quad \underline{g}(\underline{r}^* + \delta \underline{r}) = \underline{g}(\underline{r}^*) + \frac{\partial \underline{g}(\underline{r}^*)}{\partial \underline{r}^*} \delta \underline{r} + \underline{b}$$

where the vector \underline{b} represents second and higher-order terms, (this term will be considered negligible).

$$(4.4) \quad \underline{g}(\underline{r}^* + \delta \underline{r}) = \underline{g}(\underline{r}^*) + \frac{\partial \underline{g}(\underline{r}^*)}{\partial \underline{r}^*} \delta \underline{r}$$

The reference orbit itself also satisfies the equation of motion (2.1), but with $\Gamma = 0$.

Therefore, we get [Prussing, 1993 (c)] :

$$(4.5) \quad \underline{\ddot{r}}^* = \underline{g}(\underline{r}^*)$$

Substituting equation (4.4) into (4.2), we obtain :

$$(4.6) \quad \delta \underline{\ddot{r}} = \underline{g}(\underline{r}^*) + \frac{\partial \underline{g}(\underline{r}^*)}{\partial \underline{r}^*} \delta \underline{r} + \underline{\Gamma} - \underline{\ddot{r}}^*$$

and using (4.5), the equation becomes :

$$(4.7) \quad \delta \underline{\ddot{r}} = \frac{\partial \underline{g}(\underline{r}^*)}{\partial \underline{r}^*} \delta \underline{r} + \underline{\Gamma}$$

Since

$$(4.8) \quad \frac{\partial \underline{g}(\underline{r}^*)}{\partial \underline{r}^*} = G(\underline{r}^*)$$

equation (4.7) in its final form in the inertial frame can be written as :

$$(4.9) \quad \delta \underline{\ddot{r}} = G(\underline{r}^*) \delta \underline{r} + \underline{\Gamma}$$

For a circular reference orbit ($\underline{r}^* = \text{constant}$) in a rotating frame (X_R, Y_R, Z_R) described below, the matrix $G(\underline{r}^*)$ is a constant matrix that has the form :

$$(4.10) \quad G(\underline{r}^*) = \frac{\mu}{r^{*3}} \begin{bmatrix} 2 & 0 & 0 \\ 0 & -1 & 0 \\ 0 & 0 & -1 \end{bmatrix}$$

This result for the matrix $G(\underline{r}^*)$ is proved in appendix A.

A coordinate frame that rotates with the reference radius vector \underline{r}^* is a very convenient one in which to express vector components. A frame of this type is called the CW frame :

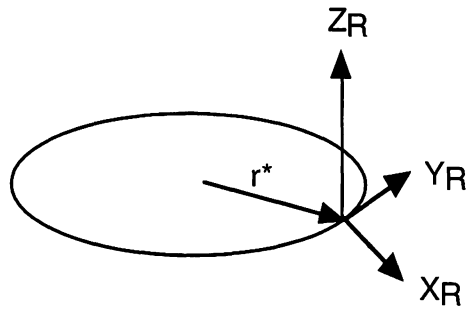


Figure 2 : Rotating frame (X_R, Y_R, Z_R)

The origin of this frame is at the reference point in the reference orbit, with the x-axis directed radially outward along the local vertical, the y-axis along the direction of motion, and the z-axis normal to the reference orbit plane.

In order to obtain the final linearized equations of relative motion for a circular reference orbit, we need to transform the acceleration $\delta \ddot{\underline{r}}$ of equation (4.9), which is relative to an observer in an inertial frame, to the acceleration $(\delta \ddot{\underline{r}})_R$, which is relative to a rotating observer fixed in the rotating frame.

The well known transformation to obtain the acceleration relative to an observer in an inertial frame is [Prussing, 1993 (c)] :

$$(4.11) \quad \delta \ddot{\underline{r}} = (\delta \ddot{\underline{r}})_R + 2\underline{w} \times (\delta \dot{\underline{r}})_R + \dot{\underline{w}} \times (\delta \underline{r})_R + \underline{w} \times (\underline{w} \times (\delta \underline{r})_R)$$

where \underline{w} represents the angular velocity of the rotating frame with respect to an inertial frame (this is the orbital angular velocity in the reference orbit).

$$(4.12) \quad \underline{w} = \begin{bmatrix} 0 \\ 0 \\ n \end{bmatrix}$$

$$(4.13) \quad n^2 = \frac{\mu}{r^{*3}}$$

$2\underline{\omega} \times (\underline{\delta \dot{r}})_R$ is the coriolis acceleration.

$\underline{\omega} \times (\underline{\omega} \times (\underline{\delta r})_R)$ is the centrifugal acceleration.

$\dot{\underline{\omega}} \times (\underline{\delta r})_R$ is the Euler acceleration.

$\underline{\delta \ddot{r}}$ is the acceleration relative to an observer in an inertial frame.

$(\underline{\delta \ddot{r}})_R$ is the acceleration relative to a rotating observer fixed in the rotating frame.

$$(4.14) \quad (\underline{\delta r})_R = \begin{bmatrix} x \\ y \\ z \end{bmatrix}$$

$$(4.15) \quad (\underline{\delta \dot{r}})_R = \begin{bmatrix} \dot{x} \\ \dot{y} \\ \dot{z} \end{bmatrix}$$

$$(4.16) \quad (\underline{\delta \ddot{r}})_R = \begin{bmatrix} \ddot{x} \\ \ddot{y} \\ \ddot{z} \end{bmatrix}$$

Substituting (4.12), (4.14), (4.15), (4.16) into (4.11), we find $\underline{\delta \ddot{r}}$ in the inertial frame :

$$(4.17) \quad \underline{\delta \ddot{r}} = \begin{bmatrix} \ddot{x} - 2n\dot{y} - n^2x \\ \ddot{y} + 2n\dot{x} - n^2y \\ \ddot{z} \end{bmatrix}$$

According to equation (4.9), the equation of motion in the rotating frame (X_R, Y_R, Z_R) is:

$$(4.18) \quad \underline{\delta \ddot{r}} = G(\underline{r}^*)(\underline{\delta r})_R + \underline{\Gamma}$$

with $G(\underline{r}^*)$ given by equation (4.10).

Developing equation (4.18), we obtain :

$$(4.19) \quad \begin{bmatrix} \ddot{x} - 2n\dot{y} - n^2x \\ \ddot{y} + 2n\dot{x} - n^2y \\ \ddot{z} \end{bmatrix} = n^2 \begin{bmatrix} 2 & 0 & 0 \\ 0 & -1 & 0 \\ 0 & 0 & -1 \end{bmatrix} \begin{bmatrix} x \\ y \\ z \end{bmatrix} + \begin{bmatrix} \Gamma_x \\ \Gamma_y \\ \Gamma_z \end{bmatrix}$$

which gives the acceleration in the rotating frame :

$$(4.20) \quad (\delta\ddot{\underline{r}})_R = \begin{bmatrix} \ddot{x} \\ \ddot{y} \\ \ddot{z} \end{bmatrix} = \begin{bmatrix} 3n^2x + 2n\dot{y} + \Gamma_x \\ -2n\dot{x} + \Gamma_y \\ -n^2z + \Gamma_z \end{bmatrix}$$

which can be written in the form :

$$(4.21) \quad (\delta\ddot{\underline{r}})_R = A \delta\underline{r} + B (\delta\dot{\underline{r}})_R + \underline{\Gamma}$$

where A is a symmetric matrix and B is skew-symmetric matrix.

$$(4.22) \quad A = \begin{bmatrix} 3n^2 & 0 & 0 \\ 0 & 0 & 0 \\ 0 & 0 & -n^2 \end{bmatrix}$$

$$(4.23) \quad B = \begin{bmatrix} 0 & 2n & 0 \\ -2n & 0 & 0 \\ 0 & 0 & 0 \end{bmatrix}$$

and

$$(4.24) \quad \underline{\Gamma} = \begin{bmatrix} \Gamma_x \\ \Gamma_y \\ \Gamma_z \end{bmatrix}$$

The details of this calculation are given in Appendix B.

The primer vector satisfies also the same equation as the variation in position

(4.21) with no thrust [Prussing, 1993 (a), (b)] :

$$(4.25) \quad \ddot{\underline{p}} = A\underline{p} + B\dot{\underline{p}}$$

A demonstration of this equation is given in Appendix C.

Knowing that equation (2.34) is :

$$\underline{\Gamma} = \underline{p}$$

and combining equations (2.34), (4.25) and (4.21), we obtain the optimal trajectory equation for a circular orbit in the CW field :

$$(4.26) \quad \delta \underline{r}^{(4)} - 2B\delta \underline{r}^{(3)} - (2A - B^2)\delta \underline{\ddot{r}} + (AB + BA)\delta \underline{\dot{r}} + A^2\delta \underline{r} = 0$$

This equation is the optimal trajectory equation of the spacecraft in the rotating frame. The details of this equation are given in Appendix D.

In order to simplify the problem, the case where the motion of all spacecraft is restricted to a plane will be treated. This is known as the coplanar case : $z=0$.

In this case, the equations of motion are :

$$(4.27) \quad \begin{aligned} x^{(4)} - 4ny^{(3)} - 10n^2\ddot{x} + 6n^3\dot{y} + 9n^4x &= 0 \\ y^{(4)} + 4nx^{(3)} - 4n^2\ddot{y} - 6n^3\dot{x} &= 0 \end{aligned}$$

with

$$(4.13) \quad n^2 = \frac{\mu}{r^*{}^3}$$

These equations are obtained in Appendix E.

4.2 Boundary conditions

For each vehicle, we have two differential equations of the fourth order and functions of x and y . These two differential equations are coupled and linear with constant coefficients. Part of the boundary conditions are at the initial time (position and velocity) and another part are at the final time (position and velocity also). Because the optimal trajectory equations found in (4.27) are in the rotating frame, the boundary conditions must also be given in the rotating frame.

The property of the rendezvous concern the final time : the position and velocity at this time must be the same for each vehicle participating in the rendezvous.

In order to find a solution $x(t)$ and $y(t)$ for each vehicle, we will transform each of the two fourth order equations in four first order equations. We obtain eight first order equations, which means that we need eight boundary conditions. As mentioned before, four of the boundary conditions will be at the initial time ($x(t_0)$, $y(t_0)$, $x'(t_0)$, $y'(t_0)$) and the other four at the final time ($x(t_f)$, $y(t_f)$, $x'(t_f)$, $y'(t_f)$).

The position of each vehicle for the initial and final times is the position of the spacecraft in the rotating frame. The velocity of each spacecraft for the initial and final times will vary with the position of the spacecraft on the orbit. These datas will be found applying (4.28) for each different cases.

$$(4.28) \quad \underline{V}_{\text{relative}} = \underline{V}_{\text{active}} - \underline{V}_{\text{rotating_frame}} - \underline{\omega} \times \underline{r}_{\text{active/rotating_frame}}$$

where :

$\underline{V}_{\text{active}}$ is the velocity of the active vehicle with respect to an inertial frame. An active vehicle is a vehicle that is using thrust for maneuvering.

$\underline{V}_{\text{rotating_frame}}$ is the velocity of the rotating frame in an inertial frame. A passive vehicle is a vehicle without thrust and therefore it will move along a fixed orbit.

$\underline{\omega}$ is the angular velocity of the rotating frame with respect to an inertial frame.

$\underline{r}_{\text{active/rotating_frame}}$ is the position of the active vehicle with respect to the rotating frame.

Let's consider the general case :

The inertial frame is a fixed frame with the origin at the center of the reference orbit (X_i, Y_i). The rotating frame (X_R, Y_R) is a frame that rotates with the passive

vehicle. Its origin is at the reference point in the reference orbit

θ is the angle of the passive vehicle in the inertial frame and φ is the angle of the active vehicle in the inertial frame. r^* is the radius of the reference orbit, which is a constant and v is the initial velocity of the active vehicle on the reference orbit and also the velocity of both passive and active vehicles at the final time. The velocity v is a constant, determined by the circular orbit, see figure 3.

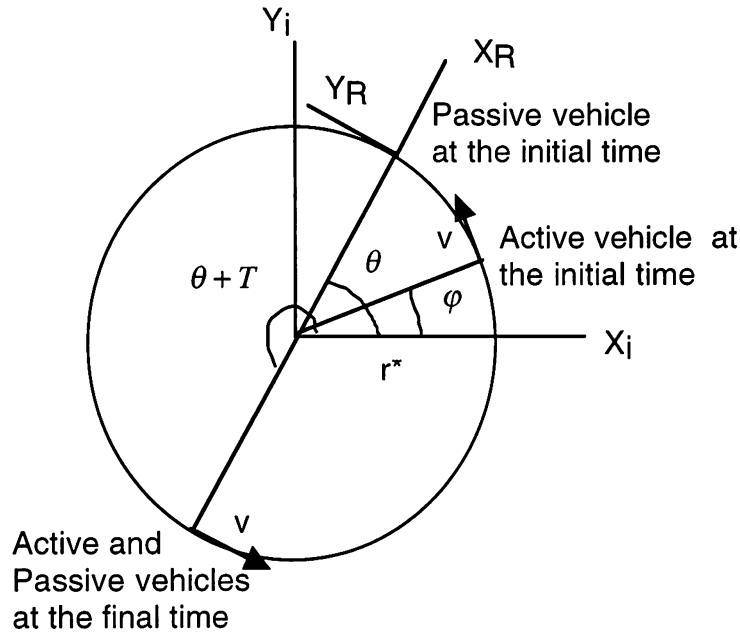


Figure 3. Position and Velocity of each spacecraft on the circular orbit in the CW field.

At the initial time to :

$$\begin{aligned}
 \underline{v}_{\text{active}} &= \begin{bmatrix} -v \cdot \sin \varphi \\ v \cdot \cos \varphi \end{bmatrix} \\
 \underline{v}_{\text{rotating_frame}} &= \begin{bmatrix} -v \cdot \sin \theta \\ v \cdot \cos \theta \end{bmatrix} \\
 \underline{r}_{\text{active/rotating_frame}} &= \begin{bmatrix} r^* \cdot (\cos(\theta - \varphi) - 1) \\ -r^* \cdot \sin(\theta - \varphi) \end{bmatrix} \\
 \underline{\omega} \times \underline{r}_{\text{active/rotating_frame}} &= \begin{bmatrix} nr^* \cdot \sin(\theta - \varphi) \\ nr^* \cdot (\cos(\theta - \varphi) - 1) \end{bmatrix} \\
 \underline{v}_{\text{relative}} &= \begin{bmatrix} v \cdot (\sin \theta - \sin \varphi) - nr^* \cdot \sin(\theta - \varphi) \\ v \cdot (\cos \varphi - \cos \theta) - nr^* \cdot (\cos(\theta - \varphi) - 1) \end{bmatrix}
 \end{aligned}
 \tag{4.29}$$

We obtain :

$$\begin{aligned}
 x(t_0) &= r^* \cdot (\cos(\theta - \varphi) - 1) \\
 y(t_0) &= -r^* \cdot \sin(\theta - \varphi) \\
 (4.30) \quad x'(t_0) &= v \cdot (\sin \theta - \sin \varphi) - nr^* \cdot \sin(\theta - \varphi) \\
 y'(t_0) &= v \cdot (\cos \varphi - \cos \theta) - nr^* \cdot (\cos(\theta - \varphi) - 1)
 \end{aligned}$$

At the final time t_f :

$$\begin{aligned}
 T &= t_f - t_0 \\
 \underline{V}_{\text{active}} &= \begin{bmatrix} -v \cdot \sin(\theta + T) \\ v \cdot \cos(\theta + T) \end{bmatrix} \\
 \underline{V}_{\text{rotating_frame}} &= \begin{bmatrix} -v \cdot \sin(\theta + T) \\ v \cdot \cos(\theta + T) \end{bmatrix} \\
 (4.31) \quad \underline{r}_{\text{active / rotating_frame}} &= \begin{bmatrix} 0 \\ 0 \end{bmatrix} \\
 \underline{\omega} \times \underline{r}_{\text{active / rotating_frame}} &= \begin{bmatrix} 0 \\ 0 \end{bmatrix} \\
 \underline{V}_{\text{relative}} &= \begin{bmatrix} 0 \\ 0 \end{bmatrix}
 \end{aligned}$$

We obtain :

$$(4.32) \quad x(t_f)=0 \quad y(t_f)=0 \quad x'(t_f)=0 \quad y'(t_f)=0$$

4.3 Transformation to inertial frame.

The optimal differential equations and the boundary conditions were given in the rotating frame but we are interested in finding the trajectory of these spacecraft in the inertial frame. So, in order to obtain the trajectories and visualize the displacement of the vehicles, we need to transform the rotating coordinates into the inertial frame.

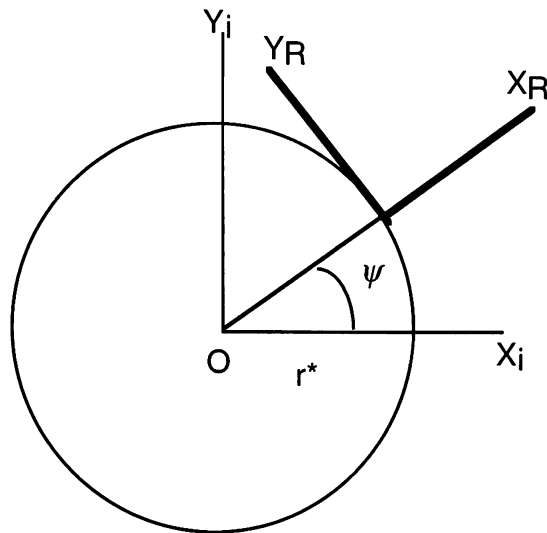


Figure 4 : Transformation from the rotating frame to the inertial frame for a circular orbit.

The axes of the rotating frame are : (X_R, Y_R, Z_R)

The axes of the inertial frame are : (X_i, Y_i, Z_i)

The planar problem is treated, therefore the vector Z_R and Z_i are the same. The angle between the rotating frame and the inertial frame is called ψ . We can transform the coordinates from the rotating frame to the inertial in two steps. The first step is to translate the coordinates $x(t)$ and $y(t)$ from the rotating frame (X_R, Y_R) in the shifted frame (X_T, Y_T) . The second step will be to rotate the shifted frame in order to obtain the equations in the inertial frame (X_i, Y_i) .

The shifted frame rotates at the same angular velocity as the rotating frame. Its center is at point O. X_T and X_R remain along the same line OX_T (or OX_R) at all times.

First Step :

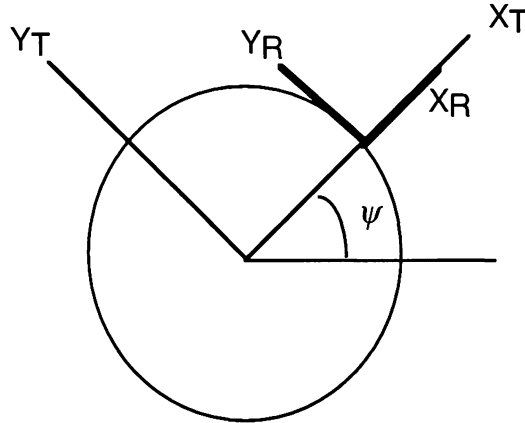


Figure 5. Transformation from the rotating frame to the shifted frame for a circular orbit.

We have the coordinates of the movement of the vehicle in the rotating frame given :

$$(4.33) \quad (\delta \underline{r})_R = \begin{bmatrix} x \\ y \end{bmatrix} \quad \text{or} \quad (\delta \underline{r})_R = x \underline{x}_R + y \underline{y}_R$$

If we apply a translation on these coordinates, we obtain :

$$(4.34) \quad (\delta \underline{r})_T = \begin{bmatrix} x + r^* \\ y \end{bmatrix} \quad \text{or} \quad (\delta \underline{r})_T = (x + r^*) \underline{x}_T + y \underline{y}_T$$

with

$$(4.35) \quad r^* = \begin{bmatrix} r^* \\ 0 \end{bmatrix}$$

Second Step :

We need now to apply the rotation in order to have the coordinates in the inertial frame (X_i, Y_i) .

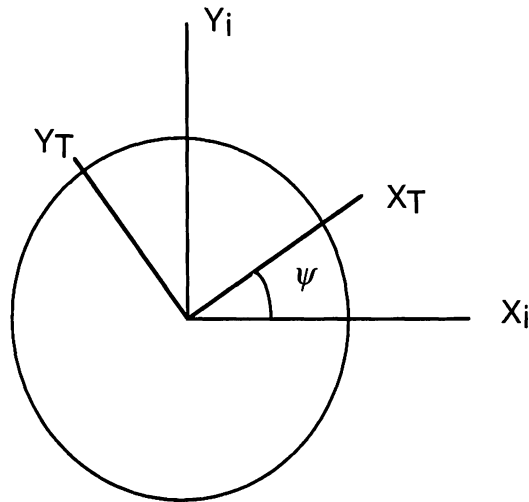


Figure 6. Transformation from the shifted frame to the inertial frame for a circular orbit.

The relations between the vectors of the shifted frame and ones of the inertial frame :

$$(4.36) \quad \begin{aligned} \underline{x}_T &= \underline{x}_i \cos \psi + \underline{y}_i \sin \psi \\ \underline{y}_T &= -\underline{x}_i \sin \psi + \underline{y}_i \cos \psi \end{aligned}$$

So the coordinates of the displacement of the vehicle of the inertial frame are :

$$(4.37) \quad \begin{aligned} (\delta \underline{r})_i &= (x + r^*) \cdot (\underline{x}_i \cos \psi + \underline{y}_i \sin \psi) + y \cdot (-\underline{x}_i \sin \psi + \underline{y}_i \cos \psi) \\ (\delta \underline{r})_i &= ((x + r^*) \cos \psi - y \sin \psi) \cdot \underline{x}_i + ((x + r^*) \sin \psi + y \cos \psi) \cdot \underline{y}_i \\ (\delta \underline{r})_i &= \begin{bmatrix} (x + r^*) \cos \psi - y \sin \psi \\ (x + r^*) \sin \psi + y \cos \psi \end{bmatrix} \end{aligned}$$

4.4 The cost

In this problem, the cost is defined as the total amount of fuel used by all the spacecraft during the optimal rendezvous maneuver.

The cost calculated in chapter 2 is :

$$J = \frac{1}{2} \int_{t_0}^{t_f} \Gamma^2(t) dt$$

Using the equation (4.21)

$$(\delta \ddot{r})_R = A \delta \dot{r} + B(\delta \dot{r})_R + \underline{\Gamma}$$

we find the coordinates of $\underline{\Gamma}(t)$ in the rotating frame.

Developing this equation for $(\delta \dot{r})_R$, we found :

$$(4.38) \quad \underline{\Gamma}(t) = \begin{bmatrix} \ddot{x} \\ \ddot{y} \\ \ddot{z} \end{bmatrix} - \begin{bmatrix} 3n^2 & 0 & 0 \\ 0 & 0 & 0 \\ 0 & 0 & -n^2 \end{bmatrix} \cdot \begin{bmatrix} x \\ y \\ z \end{bmatrix} - \begin{bmatrix} 0 & 2n & 0 \\ -2n & 0 & 0 \\ 0 & 0 & 0 \end{bmatrix} \cdot \begin{bmatrix} \dot{x} \\ \dot{y} \\ \dot{z} \end{bmatrix}$$

with x, y, z are the coordinates of $(\delta \dot{r})_R$ in the rotating frame.

$$(4.39) \quad \underline{\Gamma}(t) = \begin{bmatrix} \ddot{x} - 3n^2 x - 2n\dot{y} \\ \ddot{y} + 2n\dot{x} \\ \ddot{z} + n^2 z \end{bmatrix}$$

Considering the coplanar plane, we get :

$$(4.40) \quad \underline{\Gamma}(t) = \begin{bmatrix} \ddot{x} - 3n^2 x - 2n\dot{y} \\ \ddot{y} + 2n\dot{x} \end{bmatrix}$$

4.5 Coplanar circular rendezvous

In all our cases, we took a rendezvous duration time of $T = \Pi$.

4.5.1 Trajectories of two spacecraft in a noncooperative rendezvous

For these cases, the study will be done with the shooting method.

4.5.1.a Case 1

This case is the trivial case. The passive and the active spacecraft are at the same initial position (at a zero angle from the inertial frame ($\theta = \varphi = 0$)) and have the same velocity at the initial and final time. We obtain the following trajectories:

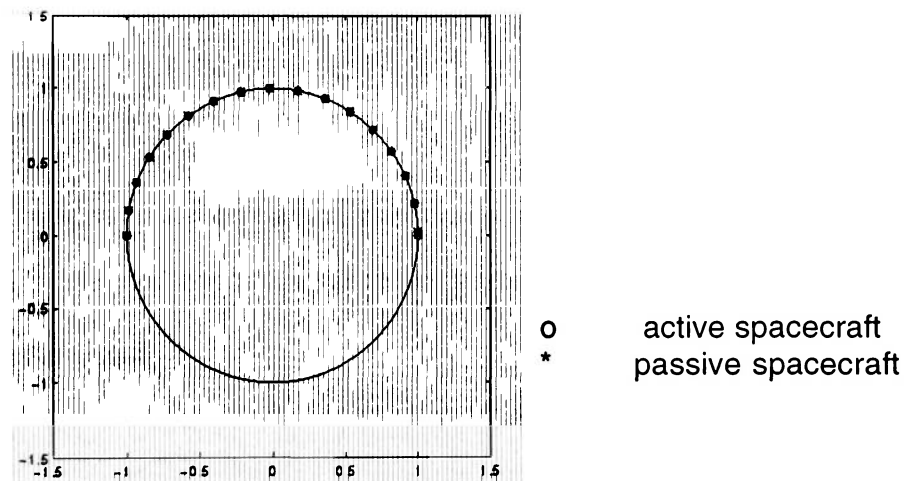


Figure 7. Spacecraft Trajectories for a circular noncooperative rendezvous : case 1.

4.5.1.b Case 2

For this case, the passive spacecraft starts at an angle $\theta = \pi/4$ of the inertial frame and the active spacecraft starts at a zero angle ($\varphi = 0$) of the inertial frame.

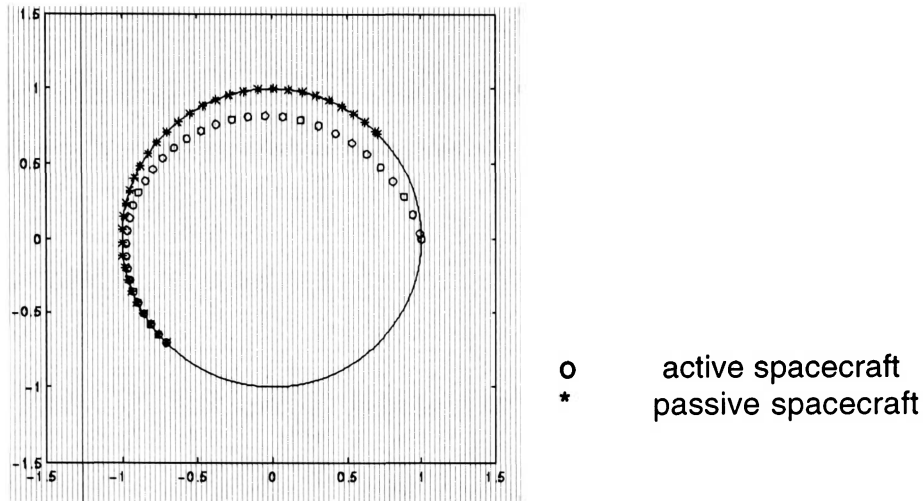


Figure 8. Spacecraft trajectories for a circular noncooperative rendezvous : case2.

4.5.1.c Case 3

In this case, the passive spacecraft starts at a zero angle compared to the inertial frame ($\theta = 0$) and the active spacecraft starts at an angle $\varphi = \pi/4$ compared to the inertial frame.

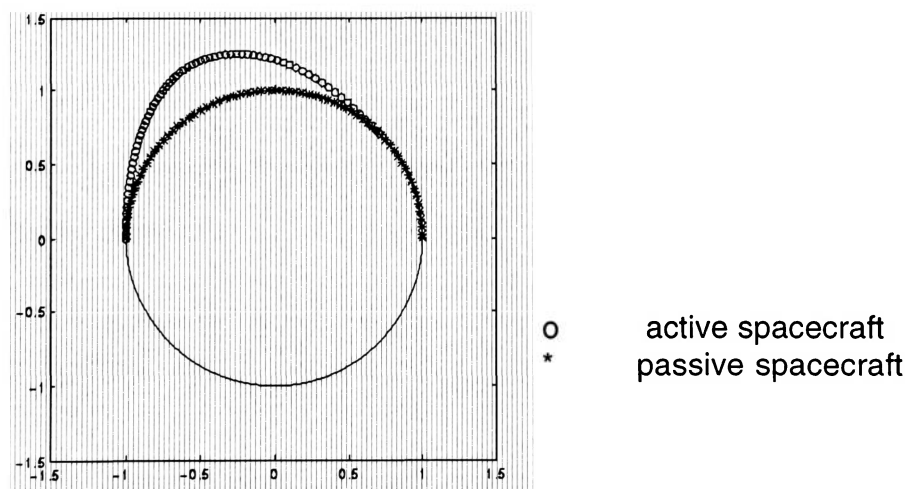


Figure 9. Spacecraft trajectories for a circular noncooperative rendezvous : case 3

4.5.2. Trajectories of the two spacecraft in a cooperative rendezvous.

For these cases, the finite difference method for linear problems was used.

4.5.2.a Case 1

In that case, the first spacecraft starts at an angle $\varphi_1 = \pi/8$ and the second spacecraft at an angle $\varphi_2 = \pi/4$ from the inertial frame. We obtain the following trajectories:

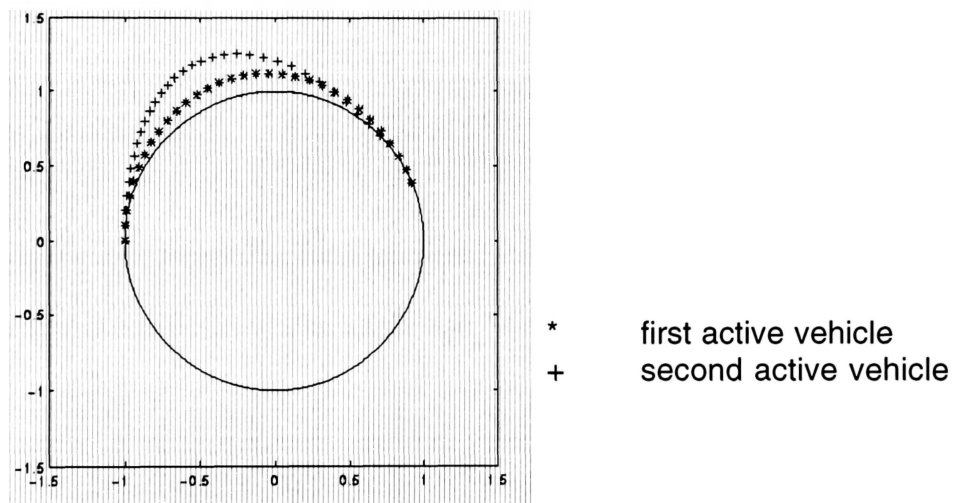


Figure 10. Spacecraft trajectories for a circular cooperative rendezvous (2 active vehicles) : case 1.

4.5.2.b Case 2

For this case, the first spacecraft starts at a zero angle of the inertial frame ($\varphi_1 = 0$) and the second spacecraft at an angle of $\varphi_2 = \pi/4$ from the inertial frame.

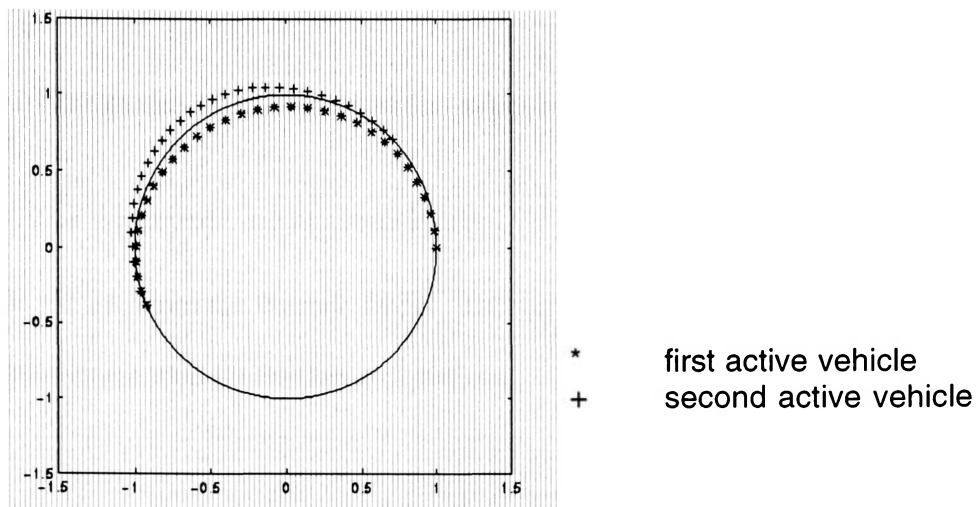


Figure 11. Spacecraft trajectories for a circular cooperative rendezvous (2 active vehicles) : case 2.

4.5.2.c Case 3

This is the case where the first spacecraft starts at a zero angle ($\varphi_1 = 0$) and the second spacecraft starts at an angle $\varphi_2 = \pi/8$.

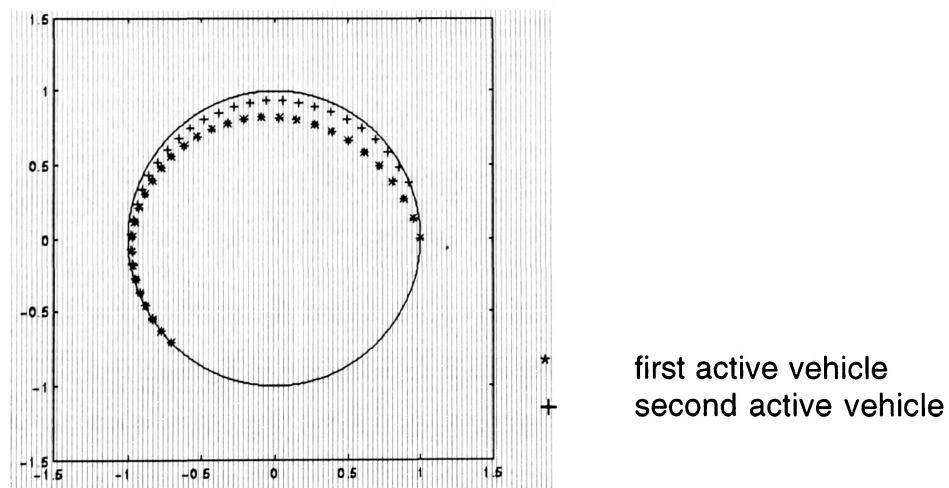


Figure 12. Spacecraft trajectories for a circular cooperative rendezvous (2 active vehicles) : case 3.

4.5.3 Trajectories of five spacecraft in a cooperative rendezvous

The five spacecraft are at respectively $\varphi_1 = 0$, $\varphi_2 = \pi/8$, $\varphi_3 = 3\pi/8$, $\varphi_4 = \pi/2$, $\varphi_5 = 5\pi/8$ from the inertial frame. The method used in this case is the finite difference method for nonlinear problems.

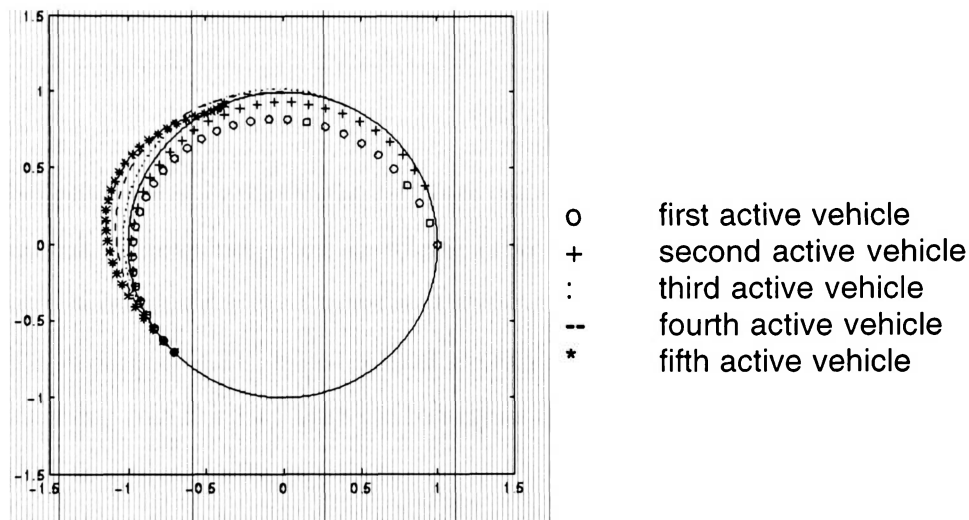


Figure 13. Spacecraft trajectories for a circular cooperative rendezvous (5 active vehicles).

4.6 Results

The rendezvous problems obtained for spacecraft neighboring a circular orbit in the CW field are linear. The three methods obtained in chapter two were used for each one of these examples. Similar trajectories were obtained for each of the three methods. However the finite differences methods (for a linear problem and a nonlinear problem) are much faster to produce the trajectories than the shooting method.

CHAPTER 5

Rendezvous of several spacecraft neighboring an elliptic orbit in the Clohessy-Wiltshire (CW) field.

This problem is similar to the problem defined in chapter 4. The only difference is that the vehicles neighbor an elliptic orbit instead of a circular one. The gravity field investigated is the Clohessy-Wiltshire field. The optimal equation in chapter four (equation (4.21)) is not correct anymore for the case of an ellipse. The theory is similar but the fact that the reference orbit is an ellipse causes a few more terms to appear in the equation.

5.1 Optimal Trajectory Equations in the CW Field.

The equations (4.1) through (4.10) are valid equations for an elliptic reference orbit. The equation of motion in the inertial frame (4.9) as well as the matrix $G(\underline{r}^*)$ given in (4.10) are :

$$(5.1) \quad \delta \ddot{\underline{r}} = G(\underline{r}^*) \delta \underline{r} + \underline{\Gamma}$$

$$(5.2) \quad G(\underline{r}^*) = \frac{\mu}{r^{*3}} \begin{bmatrix} 2 & 0 & 0 \\ 0 & -1 & 0 \\ 0 & 0 & -1 \end{bmatrix}$$

$G(\underline{r}^*)$ calculated in Appendix A is not a constant matrix anymore. It varies with \underline{r}^* given below :

$$(5.3) \quad r^* = \frac{a(1-e^2)}{1+e \cos \varphi}$$

with :

a : semimajor axis

e : eccentricity of the conic (for an ellipse = $0 < e < 1$)

φ : true anomaly.

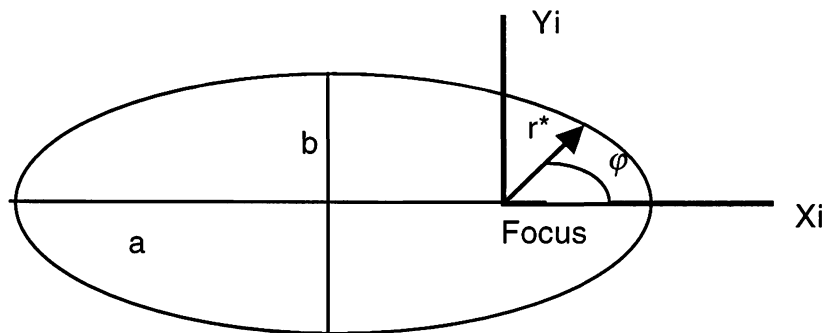


Figure 14. Elliptic orbit

For convenience we will still work in the rotating frame also called the CW frame described below :

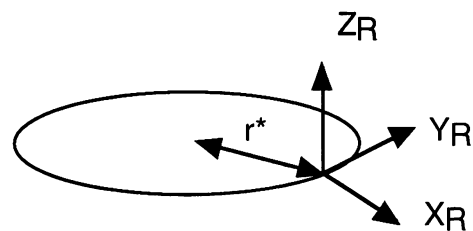


Figure 2 : Rotating frame (X_R, Y_R, Z_R)

The equation of motion in the rotating frame is found from the equation of motion in the inertial frame (5.1) :

$$(5.4) \quad \delta \ddot{\underline{r}} = G(r^*)(\delta \underline{r})_R + \underline{\Gamma}$$

with the $G(r^*)$ given by equation (5.2) and

$$(5.5) \quad (\delta \underline{r})_R = \begin{bmatrix} x \\ y \\ z \end{bmatrix}$$

Developing equation (5.4) knowing equation (5.2) and equation (5.5), we obtain :

$$(5.6) \quad \delta \ddot{\underline{r}} = \begin{bmatrix} 2n^2 x + \Gamma_x \\ -n^2 y + \Gamma_y \\ -n^2 z + \Gamma_z \end{bmatrix}$$

with

$$(5.7) \quad n^2 = \frac{\mu}{r^{*3}}$$

The well known transformation between the acceleration relative to an observer in the inertial frame and the acceleration relative to a rotating observer fixed in the rotating frame is :

$$(5.8) \quad (\delta \ddot{\underline{r}})_R = \delta \ddot{\underline{r}} - 2\underline{\omega} \times (\delta \dot{\underline{r}})_R - \dot{\underline{\omega}} \times (\delta \underline{r})_R - \underline{\omega} \times (\underline{\omega} \times (\delta \underline{r})_R)$$

where $\underline{\omega}$ represents the angular velocity of the rotating frame with respect to an inertial frame.

$$(5.9) \quad \underline{\omega} = \begin{bmatrix} 0 \\ 0 \\ n \end{bmatrix}$$

The details of each term of equation (5.8) are given in chapter 4. We have :

$$(5.10) \quad (\delta \underline{r})_R = \begin{bmatrix} x \\ y \\ z \end{bmatrix}$$

$$(5.11) \quad (\delta \dot{\underline{r}})_R = \begin{bmatrix} \dot{x} \\ \dot{y} \\ \dot{z} \end{bmatrix}$$

$$(5.12) \quad (\delta \ddot{\underline{r}})_R = \begin{bmatrix} \ddot{x} \\ \ddot{y} \\ \ddot{z} \end{bmatrix}$$

We will notice that in the case of an ellipse, r^* and v are not constant terms anymore, so $\dot{w} \neq 0$:

$$(5.13) \quad \dot{w} = \begin{bmatrix} 0 \\ 0 \\ \dot{n} \end{bmatrix}$$

with

$$(5.14) \quad \dot{n} = -\frac{3}{2} \frac{\mu}{r^{*4}} \frac{\dot{r}^*}{n}$$

The derivation of n is given in Appendix F.

Substituting (5.9), (5.10), (5.11), (5.12) and (5.13) into equation (5.8), we obtain:

$$(5.15) \quad (\delta \ddot{\underline{r}})_R = \begin{bmatrix} 3n^2 x + 2n\dot{y} + \dot{n}y + \Gamma_x \\ -2n\dot{x} - \dot{n}x + \Gamma_y \\ -n^2 z + \Gamma_z \end{bmatrix}$$

The details of the calculation are given in Appendix G.

(5.15) can be written in the form :

$$(5.16) \quad (\delta \ddot{\underline{r}})_R = A' \delta \underline{r} + B(\delta \dot{\underline{r}})_R + \underline{\Gamma}$$

with

$$(5.17) \quad A' = \begin{bmatrix} 3n^2 & \dot{n} & 0 \\ -\dot{n} & 0 & 0 \\ 0 & 0 & -n^2 \end{bmatrix}$$

$$(5.18) \quad B = \begin{bmatrix} 0 & 2n & 0 \\ -2n & 0 & 0 \\ 0 & 0 & 0 \end{bmatrix}$$

$$(5.19) \quad \underline{\Gamma} = \begin{bmatrix} \Gamma_x \\ \Gamma_y \\ \Gamma_z \end{bmatrix}$$

Decomposing $A' = A + R$, the primer vector satisfies the following equation :

$$(5.20) \quad \ddot{p} = B\dot{p} + (A - R + \dot{B})p$$

with B given (5.18) and A, R and \dot{B} given below :

$$(5.21) \quad A = \begin{bmatrix} 3n^2 & 0 & 0 \\ 0 & 0 & 0 \\ 0 & 0 & -n^2 \end{bmatrix}$$

$$(5.22) \quad R = \begin{bmatrix} 0 & \dot{n} & 0 \\ -\dot{n} & 0 & 0 \\ 0 & 0 & 0 \end{bmatrix}$$

$$(5.23) \quad \dot{B} = \begin{bmatrix} 0 & 2\dot{n} & 0 \\ -2\dot{n} & 0 & 0 \\ 0 & 0 & 0 \end{bmatrix}$$

The proof is given in Appendix H.

Knowing that equation (2.34) is :

$$\underline{\Gamma} = \underline{p}$$

and combining (2.34), (5.20) and (5.16), we obtain the optimal trajectory equation for an elliptic orbit in the CW field :

$$(5.24) \quad \delta \underline{r}^{(4)} - 2B \cdot \delta \underline{r}^{(3)} + (B^2 - A' - A + R - \dot{B}) \cdot \delta \underline{r}^{(2)} + \\ (BA' + AB - RB + \dot{B}B) \cdot \delta \underline{r} + (AA' - RA' + \dot{B}A') \cdot \delta \underline{r} = 0$$

Developing the optimal trajectory equation for the coplanar case, we obtain :

$$(5.25) \quad x^{(4)} - 4ny^{(3)} - 10n^2x^{(2)} - 2\dot{n}y^{(2)} - 4\dot{n}n\dot{x} + 6n^3\dot{y} + (9n^4 - \dot{n}^2)x + 3n^2\dot{n}y = 0 \\ y^{(4)} + 4ny^{(3)} + 2\dot{n}x^{(2)} - 4n^2y^{(2)} - 6n^3\dot{x} - 4\dot{n}ny - 3n^2\dot{n}x - \dot{n}^2y = 0$$

with n and \dot{n} described by (5.7) and (5.14).

The details of these equations are presented in Appendix I.

5.2 Boundary conditions

For each vehicle, we obtain a system of two differential equations of fourth order with x and y as unknowns. The two differential equations are coupled and linear with variable coefficients. The coefficients will vary in function of the position \underline{r}^* of the spacecraft on the elliptic reference orbit. In chapter 4, the equations had the same form but the coefficients were constants. The term n depending on \underline{r}^* is a constant term in a circular orbit. Once again, part of the boundary conditions are at the initial time and another part at the final time. The boundary conditions will be given in the rotating frame because the equations found in (5.25) are in the rotating frame. The same methods as the one in chapter 4 is applied to find the BC.

The equation (4.28) stays correct for the case of an elliptic orbit :

$$(5.26) \quad \underline{V}_{\text{relative}} = \underline{V}_{\text{active}} - \underline{V}_{\text{rotating_frame}} - \underline{\omega} \times \underline{r}_{\text{active/rotating_frame}}$$

where

$\underline{V}_{\text{active}}$ is the velocity of the active vehicle in an inertial frame.

$\underline{V}_{\text{rotating_frame}}$ is the velocity of the rotating frame in an inertial frame.

$\underline{\omega}$ is the angular velocity of the rotating frame with respect to an inertial frame.

$\underline{r}_{\text{active/rotating_frame}}$ is the position of the active vehicle with respect to the rotating frame.

The inertial frame is a fixed frame with the origin at the center of the reference orbit (X_i, Y_i) . The rotating frame (X_R, Y_R) is a frame that rotates with the passive vehicle. Its origin is at the reference point in the reference orbit

θ is the angle of the passive vehicle in the inertial frame and φ is the angle of the active vehicle in the inertial frame.

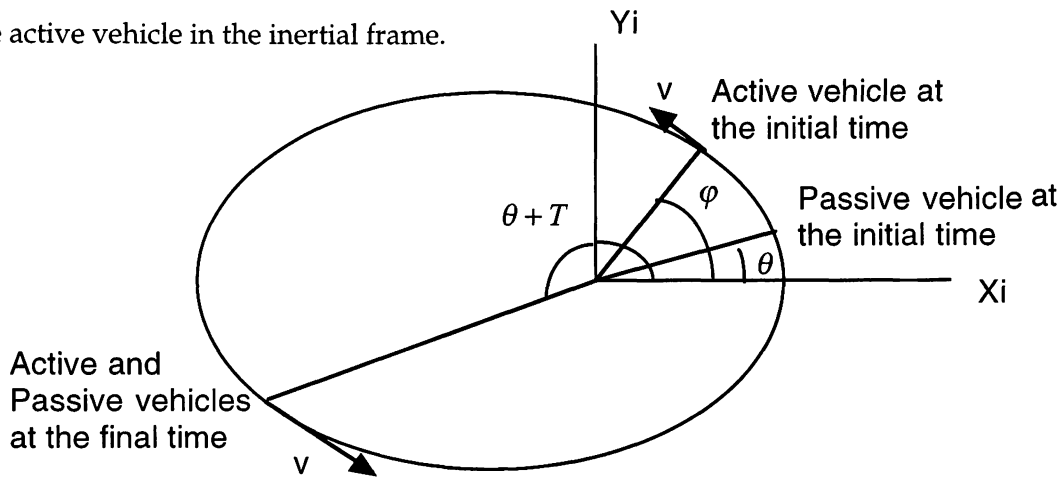


Figure 15. Position and Velocity of each spacecraft on the elliptic orbit in the CW field.

At the initial time t_0 :

$$\underline{V}_{\text{active}} = \begin{bmatrix} -v_{\text{active}} \cdot \sin \varphi \\ v_{\text{active}} \cdot \cos \varphi \end{bmatrix}$$

$$\underline{V}_{\text{rotating_frame}} = \begin{bmatrix} -v_{\text{rotating}} \cdot \sin \theta \\ v_{\text{rotating}} \cdot \cos \theta \end{bmatrix}$$

$$(5.27) \quad \underline{r}_{\text{active/rotating_frame}} = \begin{bmatrix} r_{\text{active}}^* \cdot \cos(\theta - \varphi) - r_{\text{rotating}} \\ -r_{\text{active}}^* \cdot \sin(\theta - \varphi) \end{bmatrix}$$

$$\underline{\omega} \times \underline{r}_{\text{active/rotating_frame}} = \begin{bmatrix} nr_{\text{active}}^* \cdot \sin(\theta - \varphi) \\ nr_{\text{active}}^* \cdot \cos(\theta - \varphi) - nr_{\text{rotating}} \end{bmatrix}$$

$$\underline{V}_{\text{relative}} = \begin{bmatrix} v_{\text{rotating}} \cdot \sin \theta - v_{\text{active}} \cdot \sin \varphi - nr^*_{\text{active}} \cdot \sin(\theta - \varphi) \\ v_{\text{active}} \cdot \cos \varphi - v_{\text{rotating}} \cdot \cos \theta - nr^*_{\text{active}} \cdot \cos(\theta - \varphi) + nr^*_{\text{rotating}} \end{bmatrix}$$

with:

$$v_{\text{active}} = \sqrt{\mu \left(\frac{2}{r^*_{\text{active}}} - \frac{1}{a} \right)}$$

$$v_{\text{rotating}} = \sqrt{\mu \left(\frac{2}{r^*_{\text{rotating}}} - \frac{1}{a} \right)}$$

(5.28)

$$r^*_{\text{active}} = \frac{a(1-e^2)}{1+e \cos \varphi}$$

$$r^*_{\text{rotating}} = \frac{a(1-e^2)}{1+e \cos \theta}$$

$$n^2 = \frac{\mu}{r^*_{\text{active}}{}^3}$$

The velocities are not identical anymore like in chapter four. The velocities depend on the position of the spacecraft on the ellipse radius vector \underline{r}^* .

For the initial time :

$$\begin{aligned} x(to) &= r^*_{\text{active}} \cdot \cos(\theta - \varphi) - r^*_{\text{rotating}} \\ (5.29) \quad y(to) &= -r^*_{\text{active}} \cdot \sin(\theta - \varphi) \\ x'(to) &= v_{\text{rotating}} \cdot \sin \theta - v_{\text{active}} \cdot \sin \varphi - nr^*_{\text{active}} \cdot \sin(\theta - \varphi) \\ y'(to) &= v_{\text{active}} \cdot \cos \varphi - v_{\text{rotating}} \cdot \cos \theta - nr^*_{\text{active}} \cdot \cos(\theta - \varphi) + nr^*_{\text{rotating}} \end{aligned}$$

At the final time t_f :

$$T = t_f - t_o$$

$$\underline{V}_{\text{active}} = \begin{bmatrix} -v_{\text{active}} \cdot \sin(\theta + T) \\ v_{\text{active}} \cdot \cos(\theta + T) \end{bmatrix}$$

$$(5.30) \quad \underline{V}_{\text{rotating_frame}} = \begin{bmatrix} -v_{\text{rotating}} \cdot \sin(\theta + T) \\ v_{\text{rotating}} \cdot \cos(\theta + T) \end{bmatrix}$$

$$\underline{r}_{\text{active / rotating_frame}} = \begin{bmatrix} 0 \\ 0 \end{bmatrix}$$

$$\underline{\omega} \times \underline{r}_{\text{active / rotating_frame}} = \begin{bmatrix} 0 \\ 0 \end{bmatrix}$$

$$\underline{V}_{\text{relative}} = \begin{bmatrix} 0 \\ 0 \end{bmatrix}$$

In that case, we have :

$$(5.31) \quad v_{\text{active}} = v_{\text{rotating}}$$

So, we obtain :

$$(5.32) \quad x(tf)=0 \quad y(tf)=0 \quad x'(tf)=0 \quad y'(tf)=0$$

5.3 Transformation from the rotating frame to the inertial frame

The optimal differential equations as well as the boundary conditions were given in the rotating frame. So, in order to visualize the trajectories of the spacecraft in the inertial frame, we apply the same transformation as the one found in chapter 4.

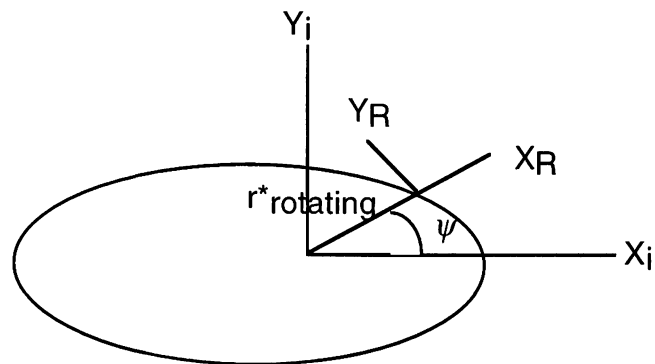


Figure 16 : Transformation from the rotating frame to the inertial frame for an elliptic orbit.

The axes of the rotating frame are : (X_R, Y_R, Z_R)

The axes of the inertial frame are : (X_i, Y_i, Z_i)

The planar case is treated, therefore the vector Z_R and Z_i are the same. We can transform the coordinates from the rotating frame to the inertial in two steps. The first step will be to translate the coordinates $x(t)$ and $y(t)$ from the rotating frame (X_R, Y_R) to the shifted frame (X_T, Y_T) . The second step will be to rotate the shifted frame to get the equations in the inertial frame (X_i, Y_i) .

First Step:

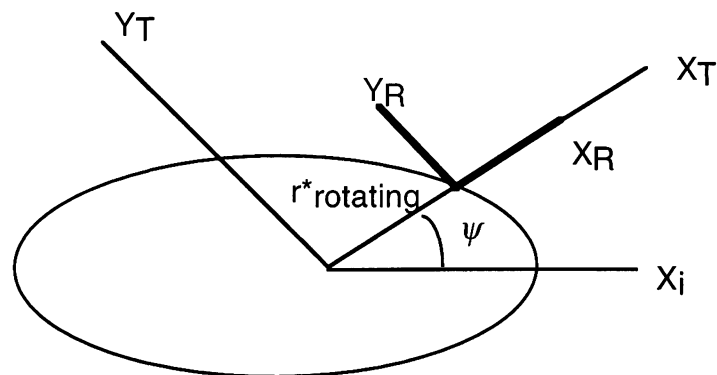


Figure 17. Transformation from the rotating frame to the shifted frame for an elliptic orbit.

We have the coordinates of the movement of the vehicle in the rotating frame given :

$$(5.33) \quad (\delta \underline{r})_R = \begin{bmatrix} x \\ y \end{bmatrix} \quad \text{or} \quad (\delta \underline{r})_R = x \underline{x}_R + y \underline{y}_R$$

If we apply a translation on these coordinates for the ellipse, we obtain :

$$(5.34) \quad (\delta \underline{r})_T = \begin{bmatrix} x + r^*_{\text{rotating}} \\ y \end{bmatrix} \quad \text{or} \quad (\delta \underline{r})_T = (x + r^*_{\text{rotating}}) \underline{x}_T + y \underline{y}_T$$

with

$$(5.35) \quad r^*_{\text{rotating}} = \frac{a(1-e^2)}{1+e \cos \psi}$$

Second Step :

We need now to apply the rotation in order to have the coordinates in the inertial frame (X_i, Y_i) .

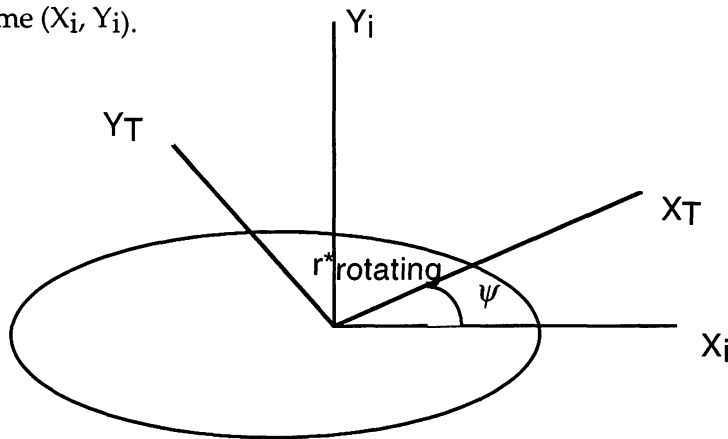


Figure 18. Transformation from the shifted frame to the inertial frame for an elliptical orbit.

The relations between the vectors of the shifted frame and ones of the inertial frame :

$$(5.36) \quad \begin{aligned} \underline{x}_r &= \underline{x}_i \cos \psi + \underline{y}_i \sin \psi \\ \underline{y}_r &= -\underline{x}_i \sin \psi + \underline{y}_i \cos \psi \end{aligned}$$

So the coordinates of the displacement of the vehicle of the inertial frame are :

$$(5.37) \quad \begin{aligned} (\delta \underline{r})_i &= (x + r^*_{\text{rotating}}) \cdot (\underline{x}_i \cos \psi + \underline{y}_i \sin \psi) + y \cdot (-\underline{x}_i \sin \psi + \underline{y}_i \cos \psi) \\ (\delta \underline{r})_i &= ((x + r^*_{\text{rotating}}) \cos \psi - y \sin \psi) \cdot \underline{x}_i + ((x + r^*_{\text{rotating}}) \sin \psi + y \cos \psi) \cdot \underline{y}_i \\ (\delta \underline{r})_i &= \begin{bmatrix} (x + r^*_{\text{rotating}}) \cos \psi - y \sin \psi \\ (x + r^*_{\text{rotating}}) \sin \psi + y \cos \psi \end{bmatrix} \end{aligned}$$

with r^*_{rotating} given by (5.35).

5.4 The cost

In this problem, the cost is defined as the total amount of fuel used by all the spacecraft during the optimal rendezvous maneuver.

The cost calculated in chapter 2 is :

$$J = \frac{1}{2} \int_{t_0}^{t_f} \Gamma^2(t) dt$$

Using the equation (5.16), we obtain the acceleration $\underline{\Gamma}(t)$:

$$(5.38) \quad \underline{\Gamma}(t) = (\delta \ddot{\underline{r}})_R - A' \delta \underline{r} - B(\delta \dot{\underline{r}})_R$$

Developping this equation, we obtain :

$$(5.39) \quad \underline{\Gamma}(t) = \begin{bmatrix} \ddot{x} \\ \ddot{y} \\ \ddot{z} \end{bmatrix} - \begin{bmatrix} 3n^2 & \dot{n} & 0 \\ -\dot{n} & 0 & 0 \\ 0 & 0 & -n^2 \end{bmatrix} \cdot \begin{bmatrix} x \\ y \\ z \end{bmatrix} - \begin{bmatrix} 0 & 2n & 0 \\ -2n & 0 & 0 \\ 0 & 0 & 0 \end{bmatrix} \cdot \begin{bmatrix} \dot{x} \\ \dot{y} \\ \dot{z} \end{bmatrix}$$

with x, y, z the coordinates of $(\delta \underline{r})_R$ in the rotating frame.

$$(5.40) \quad \underline{\Gamma}(t) = \begin{bmatrix} \ddot{x} - 3n^2 x - \dot{n} y - 2n \dot{y} \\ \ddot{y} + \dot{n} x + 2n \dot{x} \\ \ddot{z} + n^2 z \end{bmatrix}$$

For the coplanar case, we obtain :

$$(5.41) \quad \underline{\Gamma}(t) = \begin{bmatrix} \ddot{x} - 3n^2 x - \dot{n} y - 2n \dot{y} \\ \ddot{y} + \dot{n} x + 2n \dot{x} \end{bmatrix}$$

5.5 Coplanar elliptic rendezvous : trajectories of two spacecraft in a noncooperative rendezvous

Only the shooting method is used in these examples.

5.5.1.a *Case 1*

This case is the trivial case. The passive and the active spacecraft are at the same initial position (at a zero angle from the inertial frame) and have the same velocity at the initial and final time. The eccentricity is 0.5 and the period of time is Π .

We obtain the following trajectories:

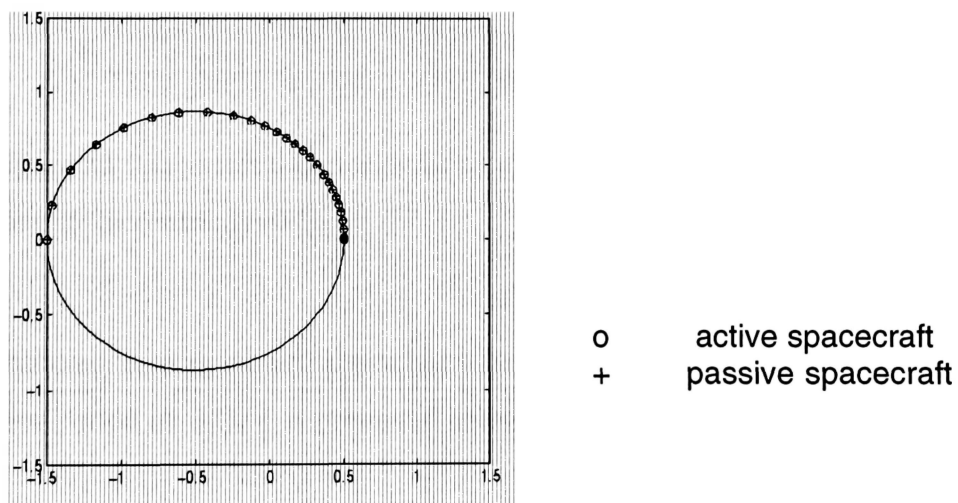


Figure 19. Spacecraft Trajectories for an elliptic noncooperative rendezvous : case 1.

5.5.1.b Case 2

For this case, the passive spacecraft starts at an angle $\theta = \pi/4$ of the inertial frame and the active spacecraft starts at a zero angle ($\varphi = 0$) of the inertial frame. The eccentricity is 0.2 and the time period is $3\pi/4$.

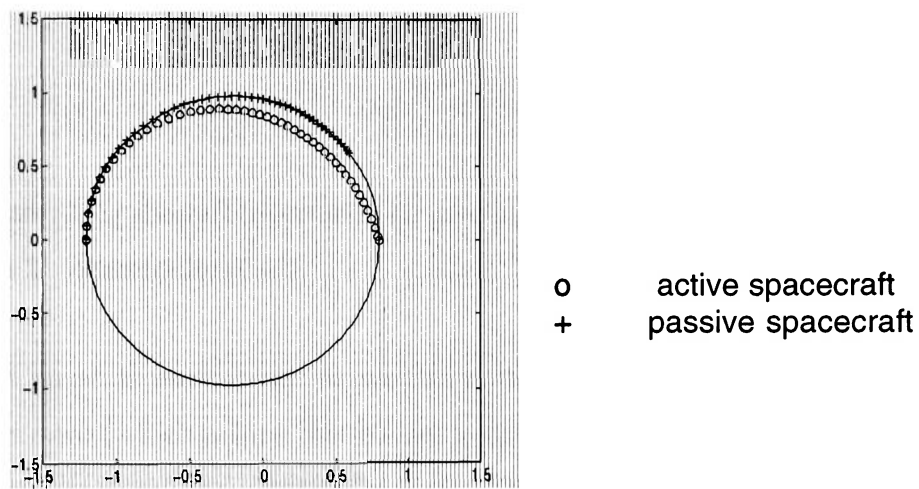


Figure 20. Spacecraft trajectories for an elliptic noncooperative rendezvous : case 2 (eccentricity=0.2).

The same case as the one above but with an eccentricity of 0.42 and an identical time period of $3\pi/4$ is presented below.

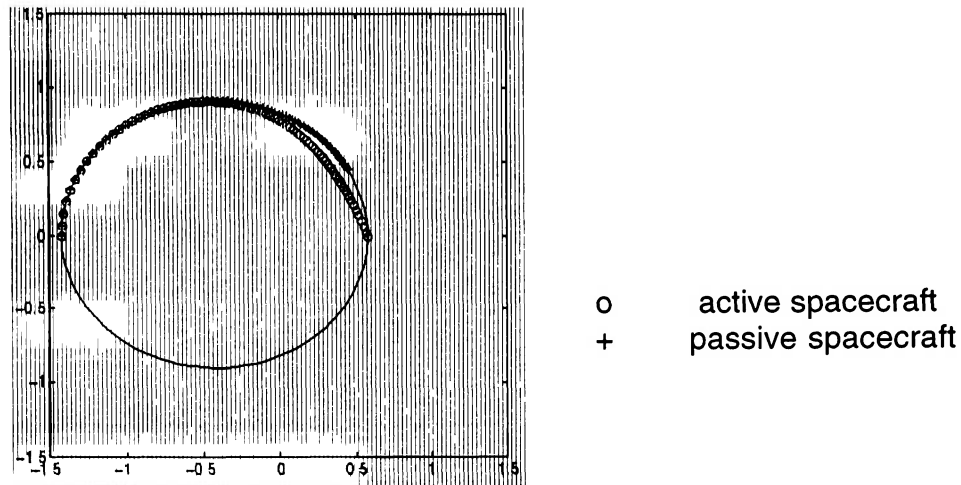


Figure 21. Spacecraft trajectories for an elliptic noncooperative rendezvous :
case 2 (eccentricity=0.42).

This graph is not correct. As we can notice, when the eccentricity became far from zero (which means that we are getting further from the circle), the initial boundary conditions became incorrect. The initial velocity is expected to be tangential to the ellipse and it is not.

5.5.1.c Case 3

This case is the case where the passive spacecraft starts at a zero angle ($\theta = 0$) compared to the inertial frame and the active spacecraft starts at an angle $\varphi = \pi/4$ compared to the inertial frame. The eccentricity is 0.2 and the time period is Π .

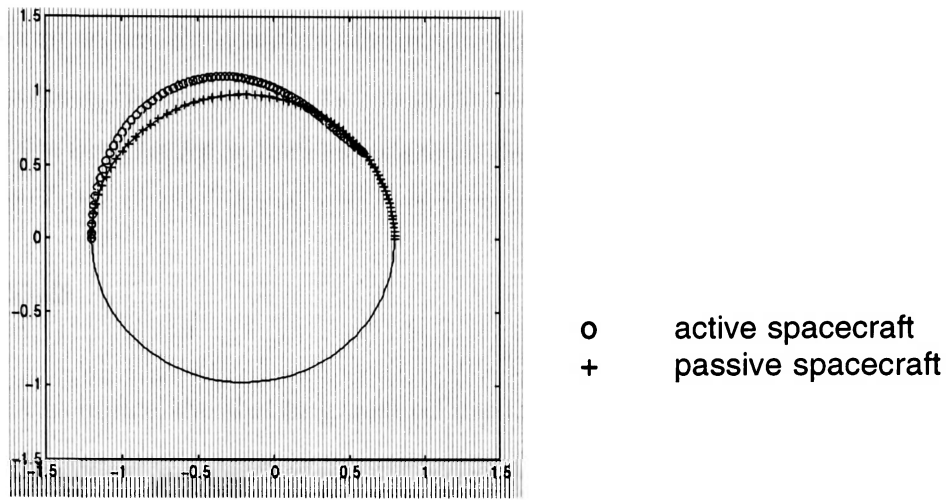


Figure 22. Spacecraft trajectories for an elliptic noncooperative rendezvous:
case 3 (eccentricity=0.2).

In order to see again the effect of the eccentricity on the spacecraft trajectories,
we increase the eccentricity to 0.4 and the time period staying the same
($T = \Pi$).

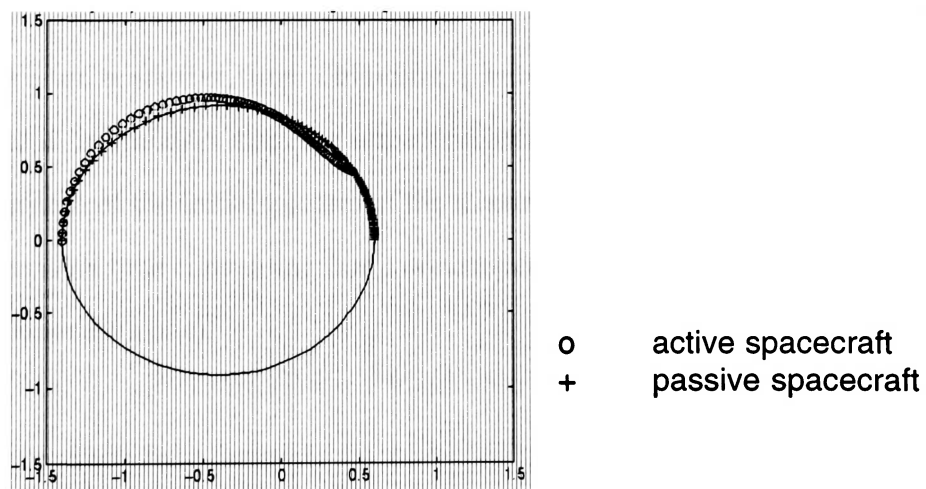


Figure 23. Spacecraft trajectories for an elliptic noncooperative rendezvous:
case 3 (eccentricity=0.4).

As we can notice, this graph is not correct either. The initial boundary conditions are incorrect. The initial velocity is expected to be tangential to the ellipse but the bigger the eccentricity is, the less tangential the initial velocity is from the ellipse.

5.6 Results

As we can notice, the shooting method used in the previous examples presents some numerical problems when the eccentricity of the ellipse is too high. The problems don't follow the boundary conditions of rendezvous problems.

The case of the cooperative rendezvous for spacecraft neighboring an elliptic orbit is not studied. The shooting method is sensitive to the initial guesses of the missing boundary conditions. If they are too far away from the solution, it will be necessary to repeat the process for another choice of initial guesses. This problem can be alleviated by solving the two point boundary value problem (TPBVP) for a shorter time, obtaining a better guess for the missing initial conditions. In the next step, the same problem is solved, but for a longer time. The research of the initial guesses of the missing boundary conditions became a problem with time consuming (for a noncooperative rendezvous and even more for a cooperative one).

The finite difference methods for linear and nonlinear problems don't work properly for the case of spacecraft neighboring an elliptic orbit. The initial boundary conditions are also incorrect on the graph. The initial velocity

of the active spacecraft should be tangential to the orbit and it is not. Two examples below are demonstrated these problems.

5.6.1 Case 1

The case where the passive spacecraft starts at a zero angle ($\theta=0$) to the inertial frame and the active spacecraft starts at an angle $\varphi = \pi/4$ to the inertial frame. The method used is the finite difference method for linear problem. The time period is Π and the eccentricity is 0.5.

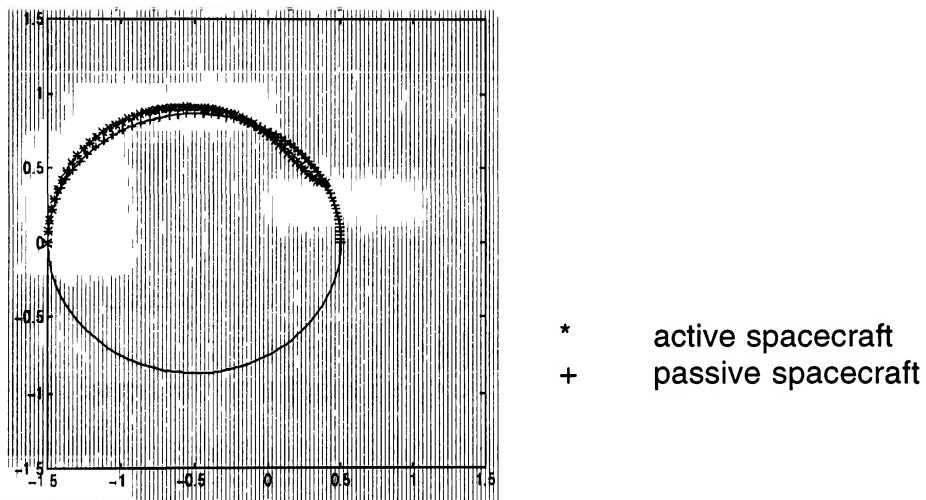


Figure 24. Spacecraft trajectories for an elliptic noncooperative rendezvous with the finite difference method for linear problems.

5.6.2 Case 2

The case where the passive spacecraft starts at an angle $\theta = \pi/4$ of the inertial frame and the active spacecraft starts at a zero angle ($\varphi = 0$) of the same frame. The method used is the finite difference method for nonlinear problem. The eccentricity is 0.5 and the time period is Π .

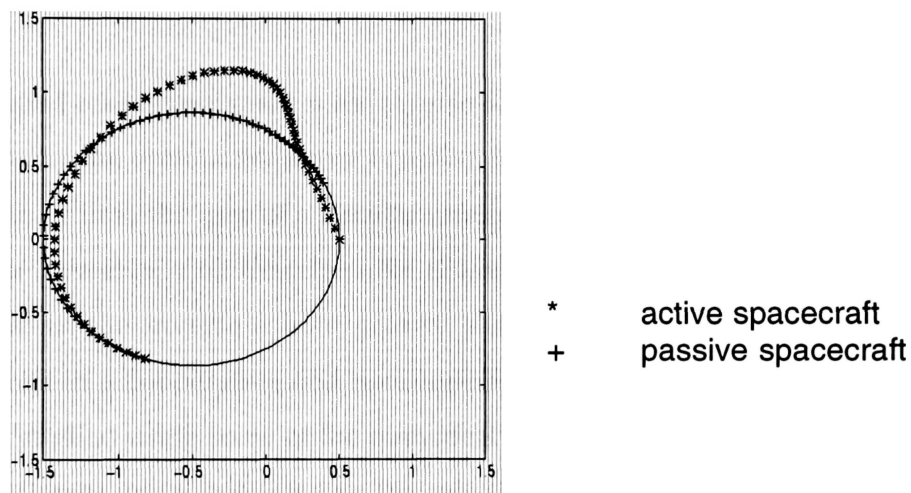


Figure 25. Spacecraft trajectories for an elliptic noncooperative rendezvous with the finite difference method for nonlinear problems.

In a future research, it would be interesting to study the trajectory of the same two problems with a smaller eccentricity for the first problem and a smaller time period for the second problem in order to see how these modifications affect the boundary conditions.

CHAPTER 6

Rendezvous of several spacecraft neighboring a circular or elliptic orbit in the Inverse-square gravity field.

The second case investigated is the inverse-square gravity field. For this case, we use directly the optimal trajectory equation found in (2.44). Like in chapter four, we treat, at first, the case of a circular reference orbit. The rendezvous problem with the reference orbit describing an ellipse is also treated in this chapter. The problem in the inverse-square gravity field was solved for more than two spacecraft in a cooperative and noncooperative rendezvous. Several examples will be studied using some of the numerical methods developed in chapter two with different initial positions on the reference orbit and different numbers of spacecraft.

6.1 Optimal Trajectory equations in the Inverse-square gravity field

From chapter 2, we use the general optimal trajectory equation (2.44) in the inertial frame for a power-limited spacecraft :

$$(6.1) \quad \underline{r}^{IV} = \dot{G}(\underline{r})\dot{\underline{r}}(t) + 2G(\underline{r})\ddot{\underline{r}}(t) - G(\underline{r})g(\underline{r})$$

where

$$(6.2) \quad \underline{r} = \begin{bmatrix} x \\ y \\ z \end{bmatrix}$$

$$(6.3) \quad g(\underline{r}) = -\mu \frac{\underline{r}}{r^3} = -\frac{\mu}{(x^2 + y^2 + z^2)^{3/2}} \begin{bmatrix} x \\ y \\ z \end{bmatrix}$$

This equation is valid for any reference orbit. The rendezvous problem in our case will be treated for either a circular or an elliptic orbit of reference.

The study is restricted to the motion in a plane ($z=0$). From Appendix J, the gravity matrix, in this case, is given by :

$$(6.4) \quad G(\underline{r}) = \begin{bmatrix} g_{xx} & g_{xy} \\ g_{yx} & g_{yy} \end{bmatrix}$$

$$(6.5) \quad \dot{G}(\underline{r}) = \begin{bmatrix} \dot{g}_{xx} & \dot{g}_{xy} \\ \dot{g}_{yx} & \dot{g}_{yy} \end{bmatrix}$$

Developping the optimal trajectory equation (5.1) for the coplanar case, we obtain :

$$(6.6) \quad \begin{aligned} x^{(4)} - 2g_{xx}\ddot{x} - 2g_{xy}\ddot{y} - \dot{g}_{xx}\dot{x} - \dot{g}_{xy}\dot{y} + g_{xx}g_x + g_{xy}g_y &= 0 \\ y^{(4)} - 2g_{yx}\ddot{x} - 2g_{yy}\ddot{y} - \dot{g}_{yx}\dot{x} - \dot{g}_{yy}\dot{y} + g_{yx}g_x + g_{yy}g_y &= 0 \end{aligned}$$

These equations are the equations of motion in the inertial frame with a reference orbit either circular or elliptic. The details of calculation concerning equations (6.3), (6.4), (6.5) and (6.6) are also given in appendix J.

6.2 Circular and Elliptic orbits

6.2.a Circular orbit

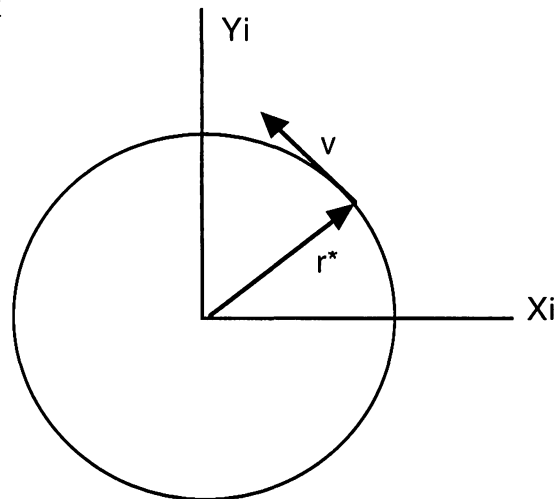


Figure 26. Circular orbit.

For that case, the radius and the velocity are constant values all along the circle :

$$(6.7) \quad \begin{aligned} r^* &= \text{const} \\ v &= \text{const} \end{aligned}$$

6.2.b Elliptic orbit

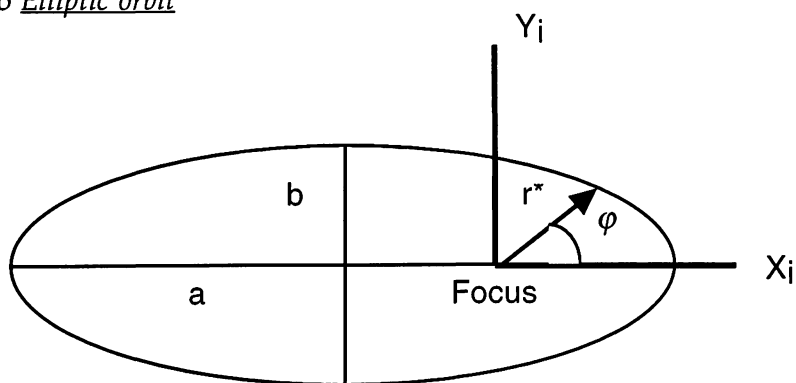


Figure 14. Elliptic orbit.

e : eccentricity of the conic; for an ellipse : $0 < e < 1$.

a : semimajor axis

φ : true anomaly

The radius r^* of an elliptic orbit is defined by :

$$(6.8) \quad r^* = \frac{a(1 - e^2)}{1 + e \cos \varphi}$$

The velocity along an elliptic orbit is variable and depends on the position of the vehicle on the orbit. The general form is obtained from vis-viva equation [Prussing, 1993 (c)].

$$(6.9) \quad v = \sqrt{\mu \left(\frac{2}{r} - \frac{1}{a} \right)}$$

6.3 Boundary conditions

For each spacecraft, we have two coupled differential equations of fourth order, for x and y . But instead of having constant coefficient like for the case of the CW field for the circular orbit in chapter four, here the coefficients are also functions of the variables x and y . This makes the problem nonlinear and more difficult to solve. Part of the boundary conditions are at the initial time and the rest at the final time. To formulate a rendezvous problem, we need to force the spacecraft to meet at the final time at the same position and velocity. The numerical methods used for the inverse-square gravity field are the ones developed in chapter two restricted to a nonlinear problem only. We will decompose the two fourth order differential equations into four first order equations. As mentioned in chapter four, we will get eight first order equations, so eight boundary conditions will be needed.

For the inverse-square gravity field problem, we worked only in the inertial frame. The initial and final positions and velocities of each spacecraft are calculated with respect to the inertial frame and no frame transformation is needed.

6.3.1 Boundary conditions for a circular orbit

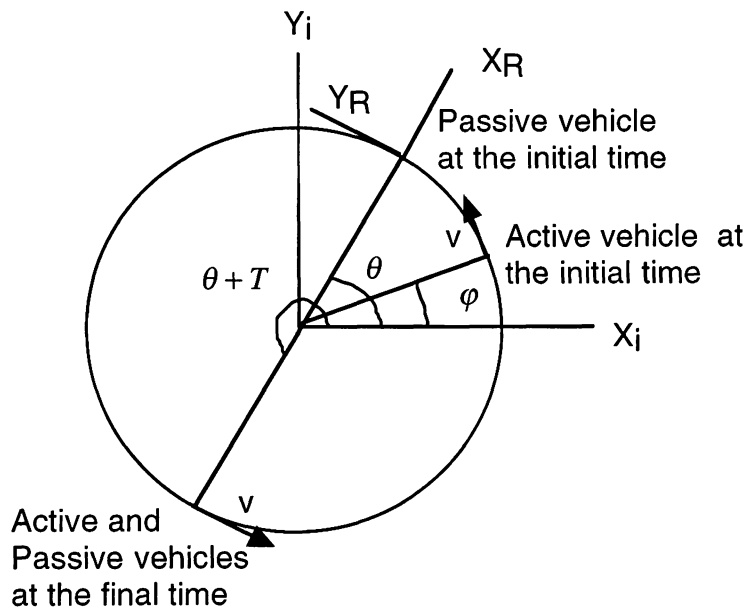


Figure 27. Position and Velocity of each spacecraft on a circular orbit in the Inverse-square gravity field.

(X_i, Y_i) unit vectors of the inertial frame.

φ : angle between the active spacecraft and the inertial frame.

θ : angle between the passive spacecraft and the inertial frame.

$T = t_f - t_0$: total time to perform the rendezvous.

	At the initial time t_0 :	At the final time t_f :
(6.10)	$x = r^* \cos \varphi$	$x = r^* \cos(\theta + T)$
	$y = r^* \sin \varphi$	$y = r^* \sin(\theta + T)$

$$\begin{aligned} x' &= -v \sin \varphi & x' &= -v \sin (\theta + T) \\ y' &= v \cos \varphi & y' &= v \cos (\theta + T) \end{aligned}$$

with $r^* = \text{constant}$ and $v = \text{constant}$.

The boundary conditions are valid if $\varphi > \theta$, $\varphi = \theta$ and $\varphi < \theta$.

6.3.2 Boundary conditions for an elliptic orbit

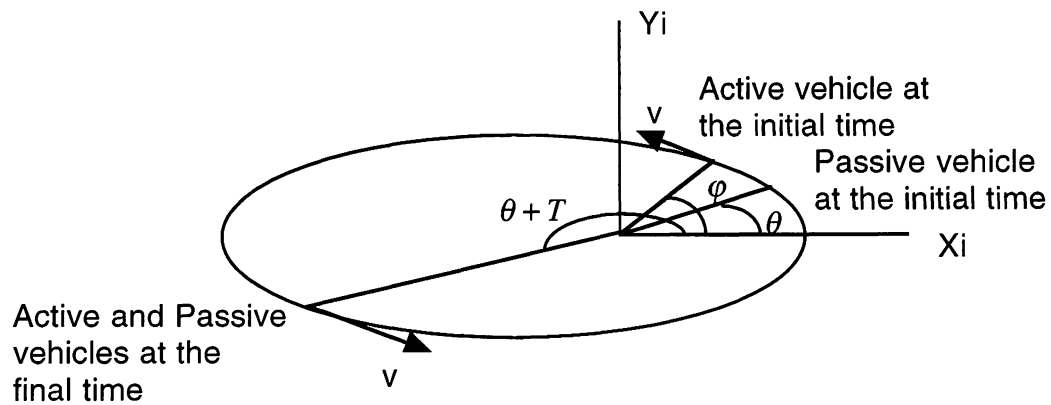


Figure 28. Position and Velocity of each spacecraft on an elliptical orbit in the Inverse-square gravity field.

(X_i, Y_i) unit vectors of the inertial frame.

φ : angle between the active spacecraft and the inertial frame.

θ : angle between the passive spacecraft and the inertial frame.

$T = t_f - t_0$: total time to perform the rendezvous.

At the initial time :

$$(6.11) \quad \begin{aligned} x &= r^*_{\text{active}} \cos \varphi \\ y &= r^*_{\text{active}} \sin \varphi \end{aligned}$$

$$x' = -v_{\text{active}} \sin \varphi$$

$$y' = v_{\text{active}} \cos \varphi$$

with :

$$r^*_{\text{active}} = \frac{a(1-e^2)}{1+e\cos\varphi}$$

(6.12)

$$v_{\text{active}} = \sqrt{\mu \left(\frac{2}{r^*_{\text{active}}} - \frac{1}{a} \right)}$$

At the final time :

$$x = r^*_{\text{active}} \cos(\theta + T)$$

$$(6.13) \quad y = r^*_{\text{active}} \sin(\theta + T)$$

$$x' = -v_{\text{active}} \sin(\theta + T)$$

$$y' = v_{\text{active}} \cos(\theta + T)$$

with :

$$r^*_{\text{active}} = \frac{a(1-e^2)}{1+e\cos(\theta+T)}$$

(6.14)

$$v_{\text{active}} = \sqrt{\mu \left(\frac{2}{r^*_{\text{active}}} - \frac{1}{a} \right)}$$

6.4 The cost

In this problem, the cost is defined as the total amount of fuel used by all the spacecraft during the optimal rendezvous maneuver.

The cost calculated in chapter two with equation (2.15) is :

$$J = \frac{1}{2} \int_{t_0}^{t_f} \Gamma^2(t) dt$$

and using the equation (3.35) :

$$\ddot{\underline{r}} = g(\underline{r}) + \underline{\Gamma}$$

we get for the coordinates of $\underline{\Gamma}(t)$ for the coplanar case :

$$(6.15) \quad \underline{\Gamma}(t) = \begin{bmatrix} \ddot{x} - g_x \\ \ddot{y} - g_y \end{bmatrix}$$

6.5 Coplanar circular rendezvous

For all the cases presented below, only the shooting method is used and the time period is Π .

6.5.1 Trajectories of two spacecraft in a noncooperative rendezvous

6.5.1.a *Case1*

This case is the trivial case. The passive spacecraft are at the same position (at a zero angle from the inertial frame) and have the same velocity at the initial and final time. We obtain the following trajectories :

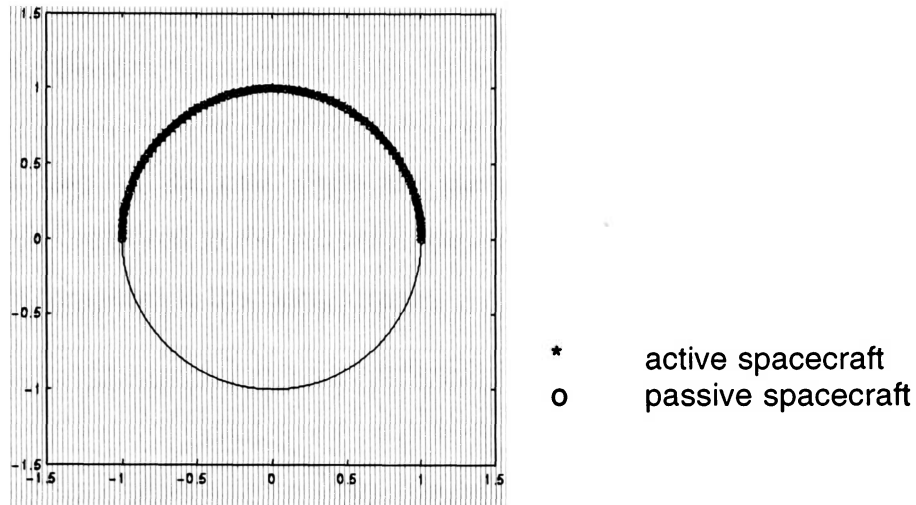


Figure 29. Spacecraft Trajectories for a circular noncooperative rendezvous :
case 1

6.5.1.b Case2

For this case, the passive spacecraft starts at an angle $\theta = \pi / 4$ of the inertial frame and the active spacecraft starts at a zero angle ($\varphi=0$) of the inertial frame.

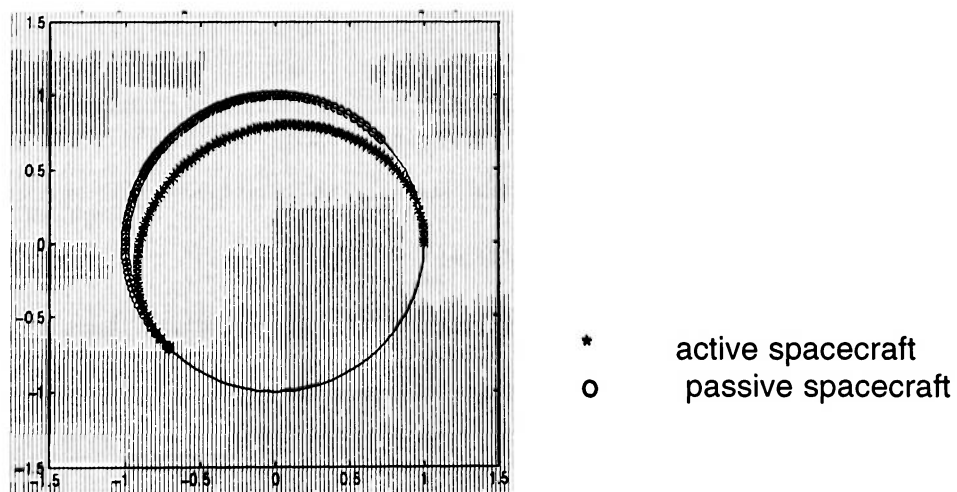


Figure 30. Spacecraft trajectories for a circular noncooperative rendezvous :
case 2.

6.5.1.c Case3

This case is the case where the passive spacecraft starts at a zero angle ($\theta=0$) compared to the inertial frame and the active spacecraft at an angle $\varphi = \pi/4$ compared to the inertial frame.

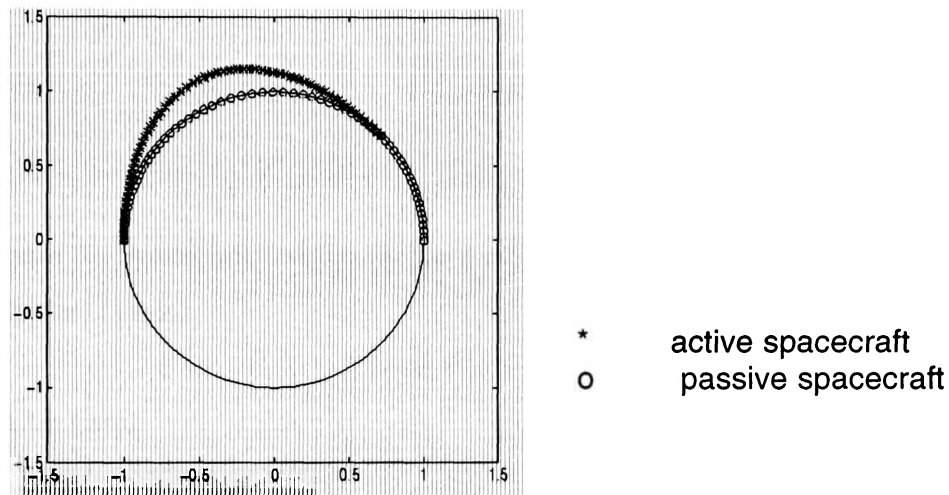


Figure 31. Spacecraft trajectories for a circular noncooperative rendezvous : case 3

6.5.2 Trajectories of two spacecraft in a cooperative rendezvous

6.5.2.a Case1

In that case, the first spacecraft starts at an angle $\varphi_1 = \pi/8$, the second spacecraft at an angle $\varphi_2 = \pi/4$ from the inertial frame. We obtain the following trajectories :

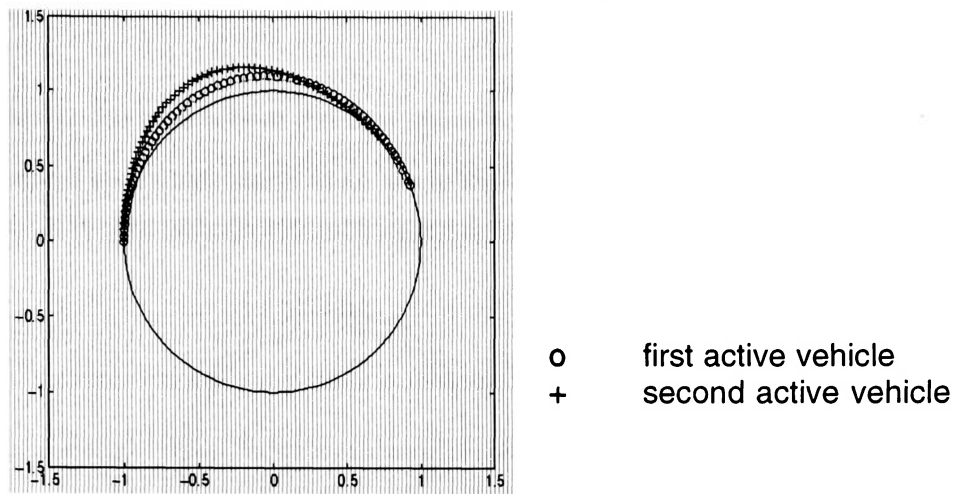


Figure 32. Spacecraft trajectories for a circular cooperative rendezvous (2 active vehicles) : case 1.

6.5.2.b Case2

For this case, the first spacecraft starts at a zero angle ($\varphi_1=0$) of the inertial frame and the second spacecraft at an angle of $\varphi_2 = \pi / 4$ from the inertial frame.

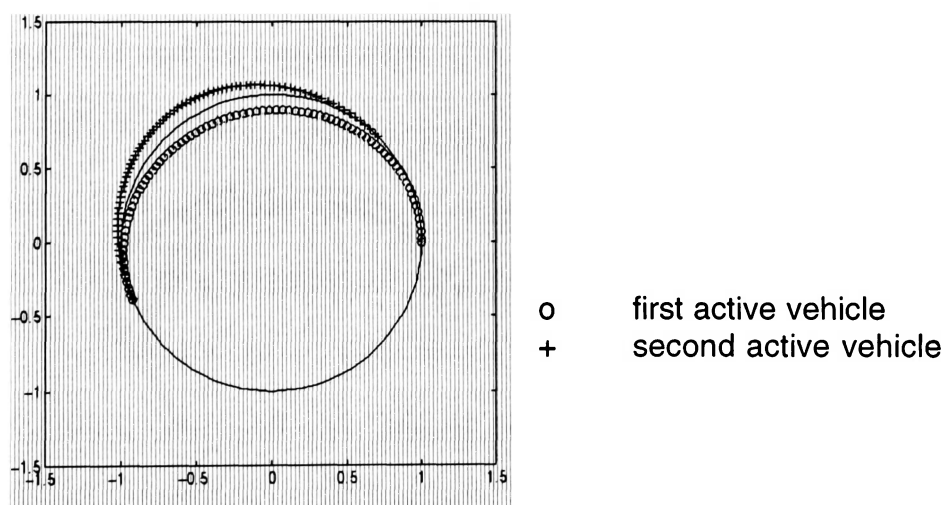


Figure 33. Spacecraft trajectories for a circular cooperative rendezvous (2 active vehicles) : case 2.

6.5.2.c Case3

This is the case where the first spacecraft starts at a zero angle ($\varphi_1=0$) and the second spacecraft starts at an angle $\varphi_2 = \pi / 8$.

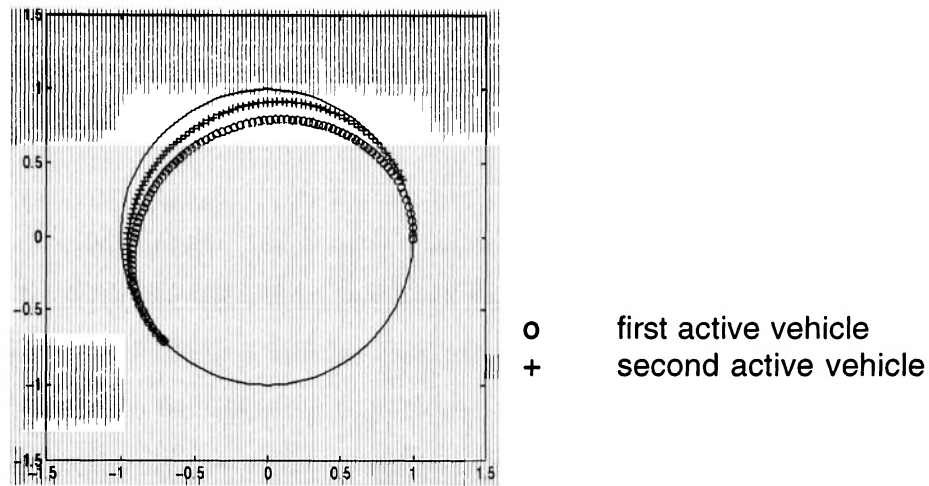


Figure 34. Spacecraft trajectories for a circular cooperative rendezvous (2 active vehicles) : case 3.

6.5.3 Trajectories of four spacecraft in a cooperative rendezvous

The four spacecraft are at respectively $\varphi_1 = 0$, $\varphi_2 = \pi / 8$, $\varphi_3 = 3 \pi / 8$ and $\varphi_4 = 5 \pi / 8$ from the inertial frame.

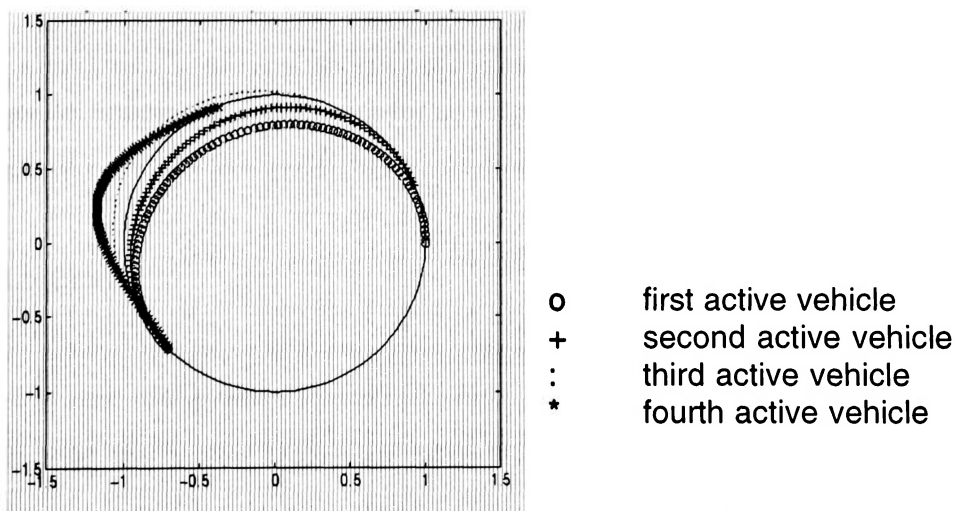


Figure 35. Spacecraft trajectories for a circular cooperative rendezvous (4 active

vehicles)

6.6 Coplanar elliptic rendezvous : trajectories of two spacecraft in a noncooperative rendezvous

For all these cases, the shooting method is the one used to solve these problems.

6.6.1.a *Case1*

This is the trivial case. The passive spacecraft are at the same position (at a zero angle from the inertial frame) and have the same velocity at the initial time and the final time. For this particular case, the eccentricity is 0.5 and the time period is Π . We obtain the following trajectories :

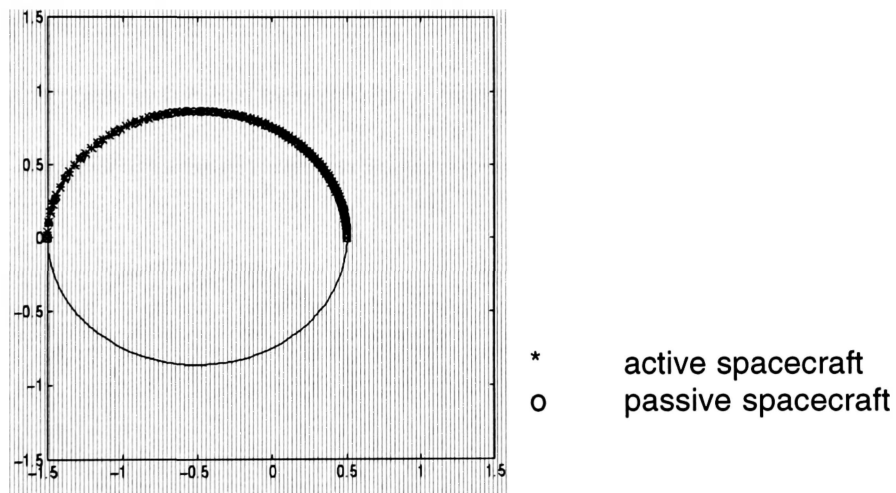


Figure 36. Spacecraft Trajectories for an elliptic noncooperative rendezvous : case 1.

6.6.1.b *Case2*

For this case, the passive spacecraft starts at an angle $\theta = \pi / 4$ of the inertial frame and the active spacecraft starts at a zero angle ($\varphi = 0$) of the inertial

frame. The period $3\Pi/4$ and the eccentricity is still 0.5.

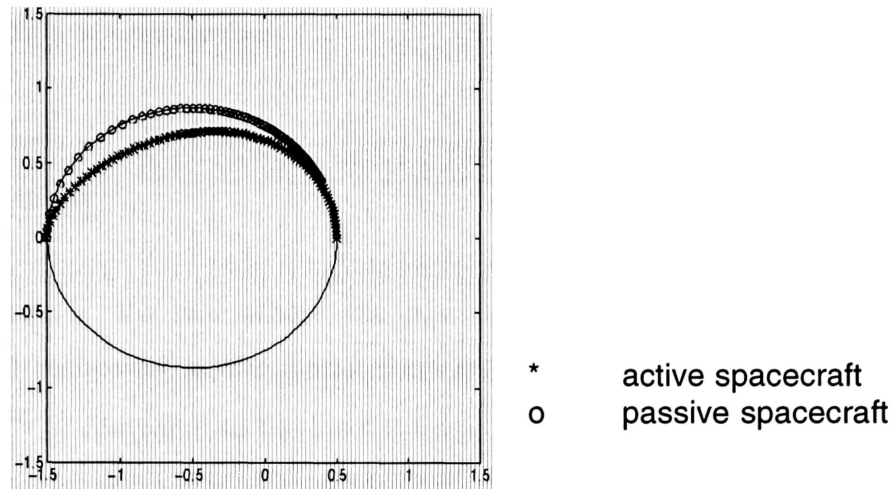


Figure 37. Spacecraft Trajectories for an elliptic noncooperative rendezvous case 2 ($T=3 \Pi/4$).

The same case is treated below with a time period of Π

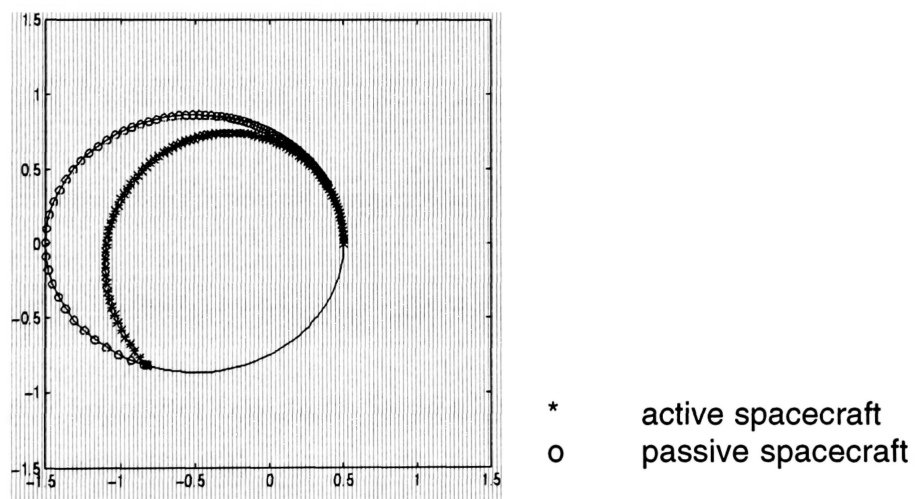


Figure 38. Spacecraft Trajectories for an elliptic noncooperative rendezvous : case 2 ($T= \Pi$).

As we can notice the final boundary conditions are incorrect. The final velocity should be tangential to the ellipse. For a too big time period, we don't get the conditions of a rendezvous.

6.6.1.c Case3

This case is the case where the passive spacecraft starts at a zero angle ($\theta = 0$) compared to the inertial frame and the active spacecraft at an angle $\varphi = \pi / 4$ compared to the inertial frame. The eccentricity is 0.2 and the time period is $T = \Pi$.

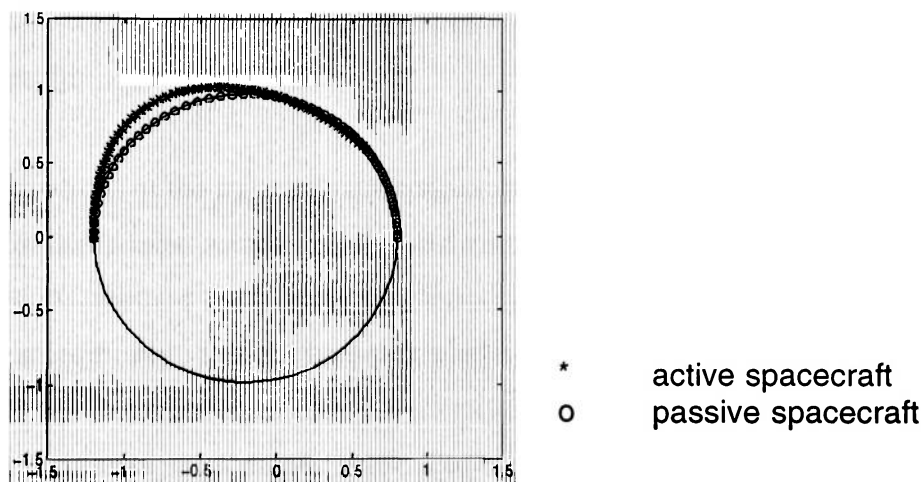


Figure 39. Spacecraft Trajectories for an elliptic noncooperative rendezvous : case 3 (eccentricity=0.2).

For the same problem, we study a bigger eccentricity (eccentricity=0.5). We notice that for this case, the initial boundary conditions are not the ones of a rendezvous because the initial velocity is not tangential to the ellipse.

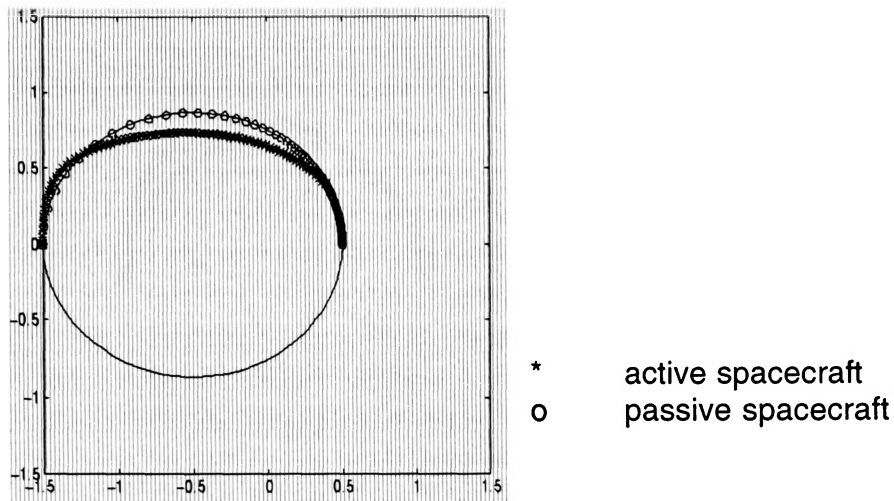


Figure 40. Spacecraft Trajectories for an elliptic noncooperative rendezvous : case 3 (eccentricity=0.5).

6.7 Results

The equations of the trajectories of spacecraft neighboring a circular or an elliptic orbit in the Inverse square gravity field are nonlinear equations. Thus, the finite difference method for a linear problem is useless in these cases. The equations were solved only with the shooting method. The finite difference method for simple nonlinear problem didn't work properly for any of those examples for either a circular or an elliptic orbit. The trajectories obtained with this method were not accurate as we can see in the following example of a noncooperative rendezvous of spacecraft neighboring a circular orbit where the passive spacecraft starts at a zero angle ($\theta = 0$) and the active spacecraft at an angle $\varphi = \pi / 4$ compared to the inertial frame.

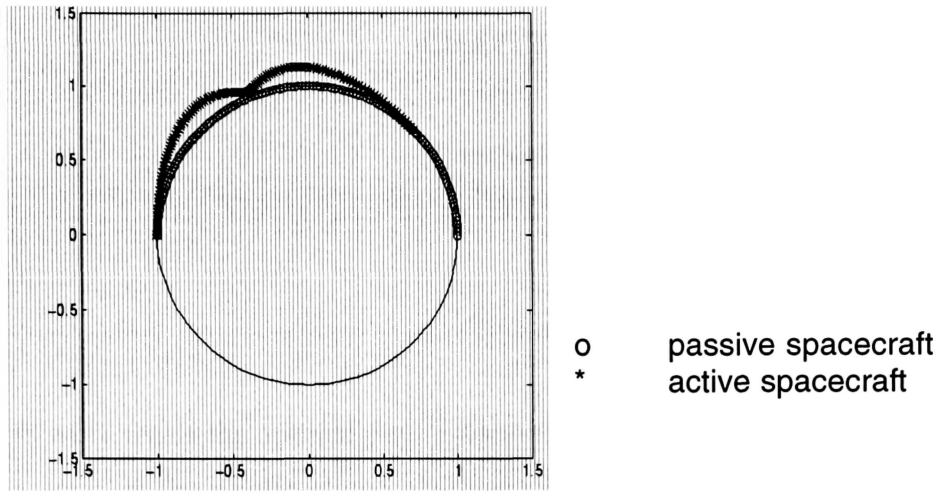


Figure 41. Spacecraft trajectories for a circular noncooperative rendezvous with the finite difference method for nonlinear problems.

The shooting method give us really good results of trajectories for the case of the circular orbit. These results are really close of the one found in the rendezvous of spacecraft neighboring the circular orbit in the Clohessy-Wiltshire field.

For the elliptic orbit problems, only the cases of the noncooperative rendezvous were treated successfully with the shooting method. However, we also note for these cases that if we take a too large time period or a too large eccentricity for the ellipse, the trajectories are incorrect. The boundary conditions for the velocity are not the one of the rendezvous (either at the initial conditions or at the final conditions).

The problem of cooperative rendezvous for spacecraft neighboring the elliptic orbit with the Inverse square gravity field was not treated. As explained in five, the shooting method is really sensitive to the initial guesses of the missing boundary conditions. If the initial guesses are too far from the missing boundary conditions, the method diverges and the trajectories are incorrect. The shooting method becomes a time consuming method for a cooperative rendezvous.

CHAPTER 7

Conclusion

This work treats the optimal power-limited rendezvous problem among several spacecraft in the neighborhood of either a circular or an elliptic orbit. This is an extension of the state of the art, where only the motion of two spacecraft about a circular orbit is considered. The method of solution is different from the direct collocation technique used by Coverstone-Carroll and Prussing. The methods are the shooting method combined with the Newton method or the Levenberg-Marquard method and the finite difference methods for linear and nonlinear problems.

The first method is applicable to both circular and elliptic reference orbits in two different gravity fields (the Clohessy-Wiltshire and the inverse square gravity fields). This numerical method used was very well adapted for all these cases because it solves boundary value problems for linear or nonlinear differential equations. But this method requires a lot of computer time, especially for the elliptic orbit problems. If the initial guesses are too far from the correct values, the problem does not converge.

The other methods studied are the finite difference methods for linear and nonlinear rendezvous problems. The first one (the linear one) was used only to treat the problems with the Clohessy-Wiltshire gravity field because the Inverse square gravity field is a nonlinear problem. The second method was used for both

gravity fields. These methods are very fast in term of computer time but were not very reliable except for the case of the Clohessy-Wiltshire gravity field with spacecraft neighboring circular orbit.

In conclusion, in the future it will be very interesting to study the cooperative rendezvous problems of spacecraft neighboring an elliptic orbit in both gravity fields (Clohessy-Wiltshire and Inverse square gravity fields) and to calculate the total cost in fuel of each of these problems. An extention of this thesis will be also to work on the rendezvous problems of spacecraft starting on orbits of different radius or eccentricity and meeting on a final one.

APPENDIX A

Calculation of the symmetric gravity gradient
matrix for the case of a circular orbit
(proof of equation (4.10)).

$$G(r) = \begin{bmatrix} \frac{\partial g_x}{\partial x} & \frac{\partial g_x}{\partial y} & \frac{\partial g_x}{\partial z} \\ \frac{\partial g_y}{\partial x} & \frac{\partial g_y}{\partial y} & \frac{\partial g_y}{\partial z} \\ \frac{\partial g_z}{\partial x} & \frac{\partial g_z}{\partial y} & \frac{\partial g_z}{\partial z} \end{bmatrix}$$

$$\underline{g}(r) = -GM \frac{r}{r^3}$$

$$\underline{g}(x, y, z) = -GM \frac{(x, y, z)}{(x^2 + y^2 + z^2)^{3/2}}$$

$$g_x = -GM \frac{x}{(x^2 + y^2 + z^2)^{3/2}}$$

$$g_y = -GM \frac{y}{(x^2 + y^2 + z^2)^{3/2}}$$

$$g_z = -GM \frac{z}{(x^2 + y^2 + z^2)^{3/2}}$$

Let's calculate the partial derivatives one by one g_x , g_y , g_z with respect of x , y , z .

$$\frac{\partial g_x}{\partial x} = -GM \left[\frac{(x^2 + y^2 + z^2)^{3/2} - 3x^2(x^2 + y^2 + z^2)^{1/2}}{(x^2 + y^2 + z^2)^3} \right]$$

$$\frac{\partial g_x}{\partial y} = 3GM \frac{xy}{(x^2 + y^2 + z^2)^{5/2}}$$

$$\frac{\partial g_x}{\partial z} = 3GM \frac{xz}{(x^2 + y^2 + z^2)^{5/2}}$$

$$\frac{\partial g_y}{\partial x} = 3GM \frac{xy}{(x^2 + y^2 + z^2)^{5/2}}$$

$$\frac{\partial g_y}{\partial y} = -GM \left[\frac{(x^2 + y^2 + z^2)^{3/2} - 3y^2(x^2 + y^2 + z^2)^{1/2}}{(x^2 + y^2 + z^2)^3} \right]$$

$$\frac{\partial g_y}{\partial z} = 3GM \frac{yz}{(x^2 + y^2 + z^2)^{5/2}}$$

$$\frac{\partial g_z}{\partial x} = 3GM \frac{xz}{(x^2 + y^2 + z^2)^{5/2}}$$

$$\frac{\partial g_z}{\partial y} = 3GM \frac{yz}{(x^2 + y^2 + z^2)^{5/2}}$$

$$\frac{\partial g_z}{\partial z} = -GM \left[\frac{(x^2 + y^2 + z^2)^{3/2} - 3z^2(x^2 + y^2 + z^2)^{1/2}}{(x^2 + y^2 + z^2)^3} \right]$$

To explicitly evaluate the elements of the gravity gradient matrix, it is convenient to express the vector components in a coordinate frame (X_g, Y_g) described below that rotates with the reference radius vector \underline{r}^* . In such a frame \underline{r}^* has the simple form :

$$\underline{r}^* = \begin{bmatrix} r^* \\ 0 \\ 0 \end{bmatrix}$$

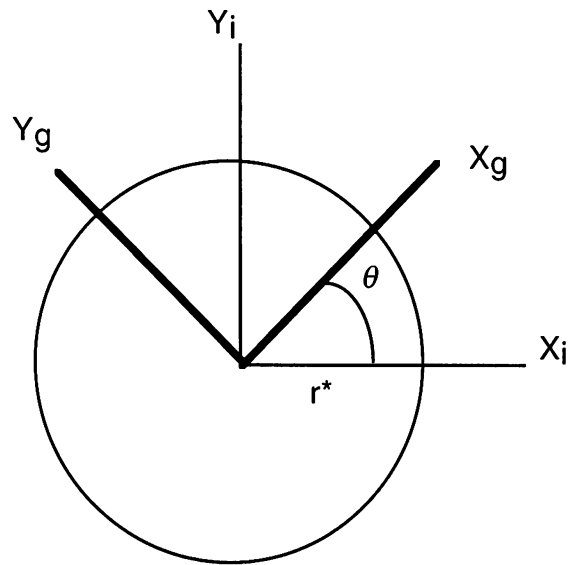


Figure A. Relation between the inertial frame and a rotating frame (X_g, Y_g).

So, in order to calculate $G(\underline{r}^*)$, we plug $x=r^*, y=z=0$. For a circular orbit, $G(\underline{r}^*)$ will remain a constant matrix because \underline{r}^* is constant along the circle. For the elliptic orbit, $G(\underline{r}^*)$ is not a constant matrix anymore, it will vary with the radius of the ellipse.

$$\frac{\partial g_x}{\partial x}(\underline{r}^*) = -GM \left[\frac{r^{*3} - 3r^{*2} r^*}{r^{*6}} \right] = \frac{2}{r^{*3}} GM$$

$$\frac{\partial g_x}{\partial y}(\underline{r}^*) = 3GM[0] = 0$$

$$\frac{\partial g_x}{\partial z}(\underline{r}^*) = 3GM[0] = 0$$

$$\frac{\partial g_y}{\partial x}(\underline{r}^*) = 3GM[0] = 0$$

$$\frac{\partial g_y}{\partial y}(\underline{r}^*) = -GM \left[\frac{r^{*3} - 0}{r^{*6}} \right] = \frac{-GM}{r^{*3}}$$

$$\frac{\partial g_y}{\partial z}(\underline{r}^*) = 3GM[0] = 0$$

$$\begin{aligned}\frac{\partial g_z}{\partial x}(\underline{r}^*) &= 3GM[0] = 0 \\ \frac{\partial g_z}{\partial y}(\underline{r}^*) &= 3GM[0] = 0 \\ \frac{\partial g_z}{\partial z}(\underline{r}^*) &= -GM \left[\frac{r^{*3} - 0}{r^{*6}} \right] = \frac{-GM}{r^{*3}}\end{aligned}$$

The matrix found is :

$$(4.10) \quad G(\underline{r}^*) = \frac{GM}{r^{*3}} \begin{bmatrix} 2 & 0 & 0 \\ 0 & -1 & 0 \\ 0 & 0 & -1 \end{bmatrix}$$

This matrix $G(\underline{r}^*)$ is valid for either circular or an elliptic orbit. The only difference is that this matrix remains constant for the circular case and vary with the position of the vehicles along the reference orbit for the elliptic case.

In this appendix, it is also important to mention that although many spacecraft are considered, the gravitational forces between the spacecraft are neglected. Only the gravitational forces between each spacecraft and the planet are taken into account.

APPENDIX B

**Calculation of the acceleration relative
to a rotating observer fixed in the CW frame
for a circular orbit
(proof of equation (4.21)).**

$$(4.11) \quad \underline{\delta \ddot{r}} = (\underline{\delta \ddot{r}})_R + 2\underline{w} \times (\underline{\delta \dot{r}})_R + (\underline{\dot{w}} \times \underline{\delta r})_R + \underline{w} \times (\underline{w} \times (\underline{\delta r})_R)$$

$$(4.12) \quad \underline{w} = \begin{bmatrix} 0 \\ 0 \\ n \end{bmatrix} \quad (4.14) \quad (\underline{\delta r})_R = \begin{bmatrix} x \\ y \\ z \end{bmatrix}$$

$$(4.15) \quad (\underline{\delta \dot{r}})_R = \begin{bmatrix} \dot{x} \\ \dot{y} \\ \dot{z} \end{bmatrix} \quad (4.16) \quad (\underline{\delta \ddot{r}})_R = \begin{bmatrix} \ddot{x} \\ \ddot{y} \\ \ddot{z} \end{bmatrix}$$

$$2\underline{w} \times (\underline{\delta \dot{r}})_R = 2 \begin{vmatrix} \underline{i} & \underline{j} & \underline{k} \\ 0 & 0 & n \\ \dot{x} & \dot{y} & \dot{z} \end{vmatrix} = 2 \begin{bmatrix} -n\dot{y} \\ nx \\ 0 \end{bmatrix}$$

$$\underline{\dot{w}} \times \underline{\delta r} = 0 \quad \text{because} \quad \underline{\dot{w}} = 0$$

$$\underline{w} \times \underline{\delta r} = \begin{vmatrix} \underline{i} & \underline{j} & \underline{k} \\ 0 & 0 & n \\ x & y & z \end{vmatrix} = \begin{bmatrix} -ny \\ nx \\ 0 \end{bmatrix}$$

$$\underline{w} \times (\underline{w} \times \underline{\delta r}) = \begin{vmatrix} \underline{i} & \underline{j} & \underline{k} \\ 0 & 0 & n \\ -ny & nx & 0 \end{vmatrix} = \begin{bmatrix} -n^2x \\ -n^2y \\ 0 \end{bmatrix}$$

Developing equation (4.11), we obtain :

$$\delta \underline{\ddot{r}} = \begin{bmatrix} \ddot{x} \\ \ddot{y} \\ \ddot{z} \end{bmatrix} + 2 \begin{bmatrix} -n\dot{y} \\ n\dot{x} \\ 0 \end{bmatrix} + \begin{bmatrix} -n^2 x \\ -n^2 y \\ 0 \end{bmatrix}$$

$$\delta \underline{\ddot{r}} = \begin{bmatrix} \ddot{x} - 2n\dot{y} - n^2 x \\ \ddot{y} + 2n\dot{x} - n^2 y \\ \ddot{z} \end{bmatrix}$$

From equation (4.9), the equation of motion in the rotating frame (X_R, Y_R, Z_R)

described below is expressed by :

$$(4.18) \quad \delta \underline{\ddot{r}} = G(\underline{r}^*)(\delta \underline{r})_R + \Gamma$$

with $G(\underline{r}^*)$ in the rotating frame given by (4.10) :

$$G(\underline{r}^*) = \frac{\mu}{r^{*3}} \begin{bmatrix} 2 & 0 & 0 \\ 0 & -1 & 0 \\ 0 & 0 & -1 \end{bmatrix}$$

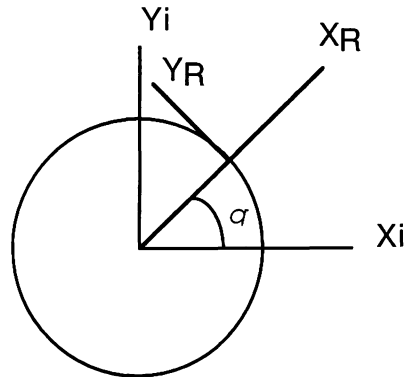


Figure 4. Transformation from the rotating frame to the inertial frame for a circular orbit.

Developing (4.18), we obtain :

$$(4.19) \quad \begin{bmatrix} \ddot{x} - 2n\dot{y} - n^2x \\ \ddot{y} + 2n\dot{x} - n^2y \\ \ddot{z} \end{bmatrix} = n^2 \begin{bmatrix} 2 & 0 & 0 \\ 0 & -1 & 0 \\ 0 & 0 & -1 \end{bmatrix} \begin{bmatrix} x \\ y \\ z \end{bmatrix} + \begin{bmatrix} \Gamma_x \\ \Gamma_y \\ \Gamma_z \end{bmatrix}$$

Putting the second derivatives in the right hand side, we obtain $(\delta\ddot{\underline{r}})_R$:

$$(4.20) \quad (\delta\ddot{\underline{r}})_R = \begin{bmatrix} \ddot{x} \\ \ddot{y} \\ \ddot{z} \end{bmatrix} = \begin{bmatrix} 3n^2x + 2n\dot{y} + \Gamma_x \\ -2n\dot{x} + \Gamma_y \\ -n^2z + \Gamma_z \end{bmatrix}$$

This equation can be written in the following form :

$$(4.21) \quad (\delta\ddot{\underline{r}})_R = A \delta\dot{\underline{r}} + B (\delta\dot{\underline{r}})_R + \underline{\Gamma}$$

with :

$$(4.22) \quad A = \begin{bmatrix} 3n^2 & 0 & 0 \\ 0 & 0 & 0 \\ 0 & 0 & -n^2 \end{bmatrix}$$

$$(4.23) \quad B = \begin{bmatrix} 0 & 2n & 0 \\ -2n & 0 & 0 \\ 0 & 0 & 0 \end{bmatrix}$$

$$(4.24) \quad \underline{\Gamma} = \begin{bmatrix} \Gamma_x \\ \Gamma_y \\ \Gamma_z \end{bmatrix}$$

APPENDIX C

Calculation of the second order primer vector differential equation for a circular orbit (proof of equation (4.25)).

The Hamiltonian for a cooperative rendezvous in the CW gravity field can be expressed from the Hamiltonian found in chapter 3 :

$$(2.22) \quad H = \frac{1}{2}\Gamma^2 + \underline{\lambda}_r^T \cdot \underline{v} + \underline{\lambda}_v^T (\underline{g} + \Gamma \underline{u})$$

Knowing that $\underline{v} = \dot{\underline{r}}$, we get :

$$H = \frac{1}{2}\Gamma^2 + \underline{\lambda}_r^T \cdot \dot{\underline{r}} + \underline{\lambda}_v^T (\underline{g}(\underline{r}) + \Gamma \underline{u})$$

and using equation (4.1)

$$\underline{r} = \delta \underline{r} + \underline{r}^* \Rightarrow \dot{\underline{r}} = \delta \dot{\underline{r}}$$

we calculate the Hamiltonian in terms of $\delta \underline{r}$:

$$H = \frac{1}{2}\Gamma^2 + \underline{\lambda}_r^T \cdot (\delta \dot{\underline{r}}) + \underline{\lambda}_v^T (g(\delta \underline{r} + \underline{r}^*) + \Gamma \underline{u})$$

with $g(\delta \underline{r} + \underline{r}^*) = A\delta \underline{r} + B(\delta \dot{\underline{r}})_R$

So, we obtain :

$$H = \frac{1}{2}\Gamma^2 + \underline{\lambda}_r^T \cdot \delta \dot{\underline{r}} + \underline{\lambda}_v^T (A\delta \underline{r} + B\delta \dot{\underline{r}} + \Gamma \underline{u})$$

Following the same procedure than the one in chapter 2, the differential equations for adjoint variables are :

$$\dot{\underline{\lambda}}_r = -\left[\frac{\partial H}{\partial \delta \underline{r}}\right]^T = -A^T \underline{\lambda}_r$$

$$\dot{\underline{\lambda}}_r = -\left[\frac{\partial H}{\partial \delta \dot{\underline{r}}}\right]^T = -(B^T \underline{\lambda}_r + \underline{\lambda}_r)$$

The primer vector was described by Lawden by equations (2.27) and (2.29) :

$$\dot{\underline{p}} = \underline{\lambda}_r$$

$$\underline{p}(t) = -\underline{\lambda}_r(t)$$

Knowing the fact that A is a symmetric matrix and B is a skew-symmetric matrix and using the two equations right above, we get :

$$\dot{\underline{\lambda}}_r = A \underline{p}$$

$$\dot{\underline{p}} = B \underline{p} + \underline{\lambda}_r$$

Differentiating the last equation with respect to time and substituting this equation in the one before last, we obtain :

$$(4.25) \quad \ddot{\underline{p}} = A \underline{p} + B \dot{\underline{p}}$$

APPENDIX D

Development of the equation
of motion in terms of $\delta \underline{r}$
for a circular orbit.

$$(4.21) \quad (\delta \ddot{\underline{r}})_r = A \delta \underline{r} + B(\delta \dot{\underline{r}})_r + \underline{\Gamma}$$

$$(4.25) \quad \ddot{\underline{p}} = A \underline{p} + B \dot{\underline{p}}$$

From (4.21)

$$\implies (*) \quad \underline{p} = \delta \ddot{\underline{r}} - A \delta \underline{r} - B \delta \dot{\underline{r}}$$

because

$$(2.34) \quad \underline{\Gamma} = \underline{p}$$

Plogging (*) in (4.25) :

$$\delta \underline{r}^{(4)} - A \delta \ddot{\underline{r}} - B \delta \underline{r}^{(3)} = A \delta \ddot{\underline{r}} - A^2 \delta \underline{r} - AB \delta \dot{\underline{r}} + B \delta \underline{r}^{(3)} - BA \delta \dot{\underline{r}} - B^2 \delta \ddot{\underline{r}}$$

$$(4.26) \quad \delta \underline{r}^{(4)} - 2B \delta \underline{r}^{(3)} - (2A - B^2) \delta \ddot{\underline{r}} + (AB + BA) \delta \dot{\underline{r}} + A^2 \delta \underline{r} = 0$$

APPENDIX E

**Development of the equation
of motion in terms of x and y
for the circular orbit.**

$$(4.26) \quad \delta \underline{r}^{(4)} - 2B\delta \underline{r}^{(3)} - (2A - B^2)\delta \underline{\ddot{r}} + (AB + BA)\delta \underline{\dot{r}} + A^2\delta \underline{r} = 0$$

$$2A - B^2 = \begin{bmatrix} 10n^2 & 0 \\ 0 & 4n^2 \end{bmatrix}$$

$$AB + BA = \begin{bmatrix} 0 & 6n^3 \\ -6n^3 & 0 \end{bmatrix}$$

$$A^2 = \begin{bmatrix} 9n^4 & 0 \\ 0 & 0 \end{bmatrix}$$

$$2B = \begin{bmatrix} 0 & 4n \\ -4n & 0 \end{bmatrix}$$

$$\delta \underline{r} = \begin{bmatrix} x \\ y \end{bmatrix}$$

So (4.26) developing for x and y becomes :

$$\begin{Bmatrix} x^{(4)} \\ y^{(4)} \end{Bmatrix} - \begin{bmatrix} 0 & 4n \\ -4n & 0 \end{bmatrix} \begin{Bmatrix} x^{(3)} \\ y^{(3)} \end{Bmatrix} - \begin{bmatrix} 10n^2 & 0 \\ 0 & 4n^2 \end{bmatrix} \begin{Bmatrix} \ddot{x} \\ \ddot{y} \end{Bmatrix} + \begin{bmatrix} 0 & 6n^3 \\ -6n^3 & 0 \end{bmatrix} \begin{Bmatrix} \dot{x} \\ \dot{y} \end{Bmatrix} + \begin{bmatrix} 9n^4 & 0 \\ 0 & 0 \end{bmatrix} \begin{Bmatrix} x \\ y \end{Bmatrix} = 0$$

$$(4.27) \quad \begin{aligned} x^{(4)} - 4ny^{(3)} - 10n^2\ddot{x} + 6n^3\dot{y} + 9n^4x &= 0 \\ y^{(4)} + 4nx^{(3)} - 4n^2\ddot{y} - 6n^3\dot{x} &= 0 \end{aligned}$$

APPENDIX F

Calculation of the derivation of n (proof of equation (5.14)).

$$(5.7) \quad n^2 = \frac{\mu}{r^{*3}}$$

Taking the derivative both side with respect to time, we obtain :

$$2n\dot{n} = -3 \frac{\mu}{r^{*4}} \dot{r}^*$$

$$(5.14) \quad \dot{n} = -\frac{3}{2} \frac{\mu}{r^{*4}} \frac{\dot{r}^*}{n}$$

APPENDIX G

**Calculation of the acceleration relative
to a rotating observer fixed in the CW frame
for an elliptic orbit
(proof of equation (5.16)).**

$$(5.8) \quad \delta \underline{\ddot{r}} = (\delta \underline{\ddot{r}})_R + 2\underline{w} \times (\delta \underline{\dot{r}})_R + (\underline{\dot{w}} \times \delta \underline{r})_R + \underline{w} \times (\underline{w} \times (\delta \underline{r})_R)$$

$$(5.9) \quad \underline{w} = \begin{bmatrix} 0 \\ 0 \\ n \end{bmatrix} \quad (5.10) \quad (\delta \underline{r})_R = \begin{bmatrix} x \\ y \\ z \end{bmatrix}$$

$$(5.11) \quad (\delta \underline{\dot{r}})_R = \begin{bmatrix} \dot{x} \\ \dot{y} \\ \dot{z} \end{bmatrix} \quad (5.12) \quad (\delta \underline{\ddot{r}})_R = \begin{bmatrix} \ddot{x} \\ \ddot{y} \\ \ddot{z} \end{bmatrix}$$

$$(5.13) \quad \underline{\dot{w}} = \begin{bmatrix} 0 \\ 0 \\ \dot{n} \end{bmatrix}$$

Plugging (5.9), (5.10), (5.11), (5.12) and (5.13) into (5.8), we obtain :

$$2\underline{w} \times (\delta \underline{\dot{r}})_R = 2 \begin{vmatrix} \underline{i} & \underline{j} & \underline{k} \\ 0 & 0 & n \\ \dot{x} & \dot{y} & \dot{z} \end{vmatrix} = 2 \begin{bmatrix} -n\dot{y} \\ nx \\ 0 \end{bmatrix}$$

$$\begin{aligned}\underline{\dot{w}} \times \underline{\delta r} &= \begin{vmatrix} i & j & k \\ 0 & 0 & \dot{n} \\ x & y & z \end{vmatrix} = \begin{bmatrix} -\dot{n}y \\ \dot{n}x \\ 0 \end{bmatrix} \\ \underline{w} \times \underline{\delta r} &= \begin{vmatrix} i & j & k \\ 0 & 0 & n \\ x & y & z \end{vmatrix} = \begin{bmatrix} -ny \\ nx \\ 0 \end{bmatrix} \\ \underline{w} \times (\underline{w} \times \underline{\delta r}) &= \begin{vmatrix} i & j & k \\ 0 & 0 & n \\ -ny & nx & 0 \end{vmatrix} = \begin{bmatrix} -n^2x \\ -n^2y \\ 0 \end{bmatrix}\end{aligned}$$

Developing equation (5.8), we obtain :

$$\begin{aligned}\underline{\delta \ddot{r}} &= \begin{bmatrix} \ddot{x} \\ \ddot{y} \\ \ddot{z} \end{bmatrix} + 2 \begin{bmatrix} -n\dot{y} \\ n\dot{x} \\ 0 \end{bmatrix} + \begin{bmatrix} -\dot{n}y \\ \dot{n}x \\ 0 \end{bmatrix} + \begin{bmatrix} -n^2x \\ -n^2y \\ 0 \end{bmatrix} \\ \underline{\delta \ddot{r}} &= \begin{bmatrix} \ddot{x} - 2n\dot{y} - \dot{n}y - n^2x \\ \ddot{y} + 2n\dot{x} + \dot{n}x - n^2y \\ \ddot{z} \end{bmatrix}\end{aligned}$$

From equation (5.4), the equation of motion in the rotating frame (X_R, Y_R, Z_R) described below is expressed by :

$$(5.4) \quad \underline{\delta \ddot{r}} = G(\underline{r}^*)(\underline{\delta r})_R + \Gamma$$

with $G(\underline{r}^*)$ in the rotating frame given by (5.2) :

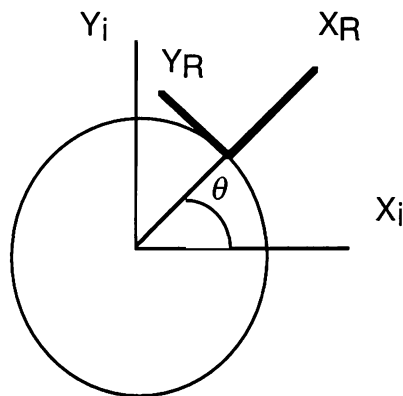


Figure 4. Transformation from the rotating frame to the inertial frame for a circular orbit.

$$(5.2) \quad G(\underline{r}^*) = \frac{\mu}{r^{*3}} \begin{bmatrix} 2 & 0 & 0 \\ 0 & -1 & 0 \\ 0 & 0 & -1 \end{bmatrix}$$

Developing (5.4), we obtain :

$$\begin{bmatrix} \ddot{x} - 2n\dot{y} - \dot{n}y - n^2x \\ \ddot{y} + 2n\dot{x} + \dot{n}x - n^2y \\ \ddot{z} \end{bmatrix} = n^2 \begin{bmatrix} 2 & 0 & 0 \\ 0 & -1 & 0 \\ 0 & 0 & -1 \end{bmatrix} \begin{bmatrix} x \\ y \\ z \end{bmatrix} + \begin{bmatrix} \Gamma_x \\ \Gamma_y \\ \Gamma_z \end{bmatrix}$$

Putting the second derivatives in the right hand side, we obtain $(\delta \underline{\ddot{r}})_R$:

$$(5.15) \quad (\delta \underline{\ddot{r}})_R = \begin{bmatrix} \ddot{x} \\ \ddot{y} \\ \ddot{z} \end{bmatrix} = \begin{bmatrix} 3n^2x + 2n\dot{y} + \dot{n}y + \Gamma_x \\ -2n\dot{x} - \dot{n}x + \Gamma_y \\ -n^2z + \Gamma_z \end{bmatrix}$$

This equation can be written in the following form :

$$(5.16) \quad (\delta \underline{\ddot{r}})_R = A' \delta \underline{r} + B (\delta \underline{\dot{r}})_R + \underline{\Gamma}$$

with :

$$(5.17) \quad A = \begin{bmatrix} 3n^2 & \dot{n} & 0 \\ -\dot{n} & 0 & 0 \\ 0 & 0 & -n^2 \end{bmatrix}$$

$$(5.18) \quad B = \begin{bmatrix} 0 & 2n & 0 \\ -2n & 0 & 0 \\ 0 & 0 & 0 \end{bmatrix}$$

$$(5.19) \quad \underline{\Gamma} = \begin{bmatrix} \Gamma_x \\ \Gamma_y \\ \Gamma_z \end{bmatrix}$$

APPENDIX H

Calculation of the second order primer vector differential equation for an elliptic orbit (proof of equation (5.20)).

The Hamiltonian for a cooperative rendezvous in the CW gravity field can be expressed from the Hamiltonian found in chapter 2 :

$$(2.22) \quad H = \frac{1}{2} \Gamma^2 + \underline{\lambda}_r^T \cdot \underline{v} + \underline{\lambda}_v^T (\underline{g} + \Gamma \underline{u})$$

Knowing that $\underline{v} = \dot{\underline{r}}$, we get :

$$H = \frac{1}{2} \Gamma^2 + \underline{\lambda}_r^T \cdot \dot{\underline{r}} + \underline{\lambda}_v^T (\underline{g}(\underline{r}) + \Gamma \underline{u})$$

and using equation (4.1) still valid for the elliptic case :

$$\underline{r} = \delta \underline{r} + \underline{r}^* \quad \Rightarrow \quad \dot{\underline{r}} = \delta \dot{\underline{r}} + \dot{\underline{r}}^*$$

we calculate the Hamiltonian in terms of $d\underline{r}$:

$$H = \frac{1}{2} \Gamma^2 + \underline{\lambda}_r^T \cdot (\delta \dot{\underline{r}} + \dot{\underline{r}}^*) + \underline{\lambda}_v^T (g(\delta \underline{r} + \underline{r}^*) + \Gamma \underline{u})$$

with

$$g(\delta \underline{r} + \underline{r}^*) = A' \delta \underline{r} + B(\delta \dot{\underline{r}})_R$$

So, we obtain :

$$H = \frac{1}{2} \Gamma^2 + \underline{\lambda}_r^T \cdot \delta \dot{\underline{r}} + \underline{\lambda}_r^T \cdot \dot{\underline{r}}^* + \underline{\lambda}_v^T (A' \delta \underline{r} + B \delta \dot{\underline{r}} + \Gamma)$$

Following the same procedure than the one in chapter three, the differential equations for adjoint variables are :

$$\dot{\underline{\lambda}}_r = - \left[\frac{\partial H}{\partial \delta \underline{r}} \right]^T = -A'^T \underline{\lambda}_r$$

$$\dot{\underline{\lambda}}_r = - \left[\frac{\partial H}{\partial \delta \dot{r}} \right]^T = -(B^T \underline{\lambda}_r + \underline{\lambda}_r)$$

The primer vector was described by Lawden by equations (2.27) and (2.29) :

$$\underline{\dot{p}} = \underline{\lambda}_r$$

$$\underline{p}(t) = -\underline{\lambda}_r(t)$$

Decomposing A' in $A+R$, with A , a symmetric matrix and R and B two skew-symmetric matrices and using the two equations right above, we get :

$$\dot{\underline{\lambda}}_r = (A - R)p$$

$$\dot{\underline{p}} = B\underline{p} + \underline{\lambda}_r$$

Differentiating the last equation with respect to time and substituting this equation in the one before last, we obtain :

$$(5.20) \quad \ddot{\underline{p}} = B\dot{\underline{p}} + (A - R + \dot{B})p$$

APPENDIX I

**Development of the equation
of motion in terms of $\delta \underline{r}$
for an elliptic orbit.**

$$(5.16) \quad (\delta \ddot{\underline{r}})_r = A' \delta \underline{r} + B(\delta \dot{\underline{r}})_r + \underline{\Gamma}$$

$$(5.20) \quad \ddot{p} = B\dot{p} + (A - R + \dot{B})p$$

From (5.16)

$$\implies (*) \quad p = \delta \ddot{r} - A' \delta r - B \delta \dot{r}$$

because

$$(2.34) \quad \underline{\Gamma} = \underline{p}$$

Plogging (*) in (5.16) :

$$\begin{aligned} \delta \underline{r}^{(4)} - A' \delta \underline{r}^{(2)} - B \delta \underline{r}^{(3)} &= B(\delta \underline{r}^{(3)} - A' \delta \dot{\underline{r}} - B \delta \underline{r}^{(2)}) \\ &+ (A - R + \dot{B})(\delta \underline{r}^{(2)} - A' \delta \underline{r} - B \delta \dot{\underline{r}}) \end{aligned}$$

$$(5.24) \quad \begin{aligned} \delta \underline{r}^{(4)} - 2B \cdot \delta \underline{r}^{(3)} + (B^2 - A' - A + R - \dot{B}) \cdot \delta \underline{r}^{(2)} + \\ (BA' + AB - RB + \dot{B}B) \cdot \delta \dot{\underline{r}} + (AA' - RA' + \dot{B}A') \cdot \delta \underline{r} = 0 \end{aligned}$$

Developing the optimal trajectory equation in the coplanar case :

$$-2B = \begin{bmatrix} 0 & -4n \\ 4n & 0 \end{bmatrix}$$

$$B^2 = \begin{bmatrix} -4n^2 & 0 \\ 0 & -4n^2 \end{bmatrix}$$

$$B^2 - A' - A + R - \dot{B} = \begin{bmatrix} -10n^2 & -2\dot{n} \\ 2\dot{n} & -4n^2 \end{bmatrix}$$

$$BA' = \begin{bmatrix} -2\dot{n}n & 0 \\ -6n^3 & -2\dot{n}n \end{bmatrix}$$

$$AB = \begin{bmatrix} 0 & 6n^3 \\ 0 & 0 \end{bmatrix}$$

$$RB = \begin{bmatrix} -2\dot{n}n & 0 \\ 0 & -2\dot{n}n \end{bmatrix}$$

$$\dot{B}B = \begin{bmatrix} -4\dot{n}n & 0 \\ 0 & -4\dot{n}n \end{bmatrix}$$

$$BA' + AB - RB + \dot{B}B = \begin{bmatrix} -4\dot{n}n & 6n^3 \\ -6n^3 & -4\dot{n}n \end{bmatrix}$$

$$AA' = \begin{bmatrix} 9n^4 & 3n^2\dot{n} \\ 0 & 0 \end{bmatrix}$$

$$RA' = \begin{bmatrix} -\dot{n}^2 & 0 \\ -3n^2\dot{n} & -\dot{n}^2 \end{bmatrix}$$

$$\dot{B}A' = \begin{bmatrix} -2\dot{n}^2 & 0 \\ -6n^2\dot{n} & -2\dot{n}^2 \end{bmatrix}$$

$$AA' - RA' + \dot{B}A' = \begin{bmatrix} 9n^4 - \dot{n}^2 & 3n^2\dot{n} \\ -3n^2\dot{n} & -\dot{n}^2 \end{bmatrix}$$

$$\begin{aligned} & \begin{Bmatrix} x^{(4)} \\ y^{(4)} \end{Bmatrix} + \begin{bmatrix} 0 & -4n \\ 4n & 0 \end{bmatrix} \begin{Bmatrix} x^{(3)} \\ y^{(3)} \end{Bmatrix} + \begin{bmatrix} -10n^2 & -2\dot{n} \\ 2\dot{n} & -4n^2 \end{bmatrix} \begin{Bmatrix} x^{(2)} \\ y^{(2)} \end{Bmatrix} + \\ & \begin{bmatrix} -4\dot{n}n & 6n^3 \\ -6n^3 & -4\dot{n}n \end{bmatrix} \begin{Bmatrix} \dot{x} \\ \dot{y} \end{Bmatrix} + \begin{bmatrix} 9n^4 - \dot{n}^2 & 3n^2\dot{n} \\ -3n^2\dot{n} & -\dot{n}^2 \end{bmatrix} \begin{Bmatrix} x \\ y \end{Bmatrix} = 0 \end{aligned}$$

$$x^{(4)} - 4ny^{(3)} - 10n^2x^{(2)} - 2\dot{n}y^{(2)} - 4\dot{n}n\dot{x} + 6n^3\dot{y} + (9n^4 - \dot{n}^2)x + 3n^2\dot{n}y = 0$$

$$y^{(4)} + 4ny^{(3)} + 2\dot{n}x^{(2)} - 4n^2y^{(2)} - 6n^3\dot{x} - 4\dot{n}n\dot{y} - 3n^2\dot{n}x - \dot{n}^2y = 0$$

APPENDIX J

Calculation of the optimal trajectory equation (6.6) for spacecraft neighboring a circular or elliptic orbit in an Inverse-square gravity field.

In this appendix, the gravitational forces between the spacecraft are neglected, only the gravitational forces between each spacecraft and the planet are taken into account.

$$(6.3) \quad g(\underline{r}) = -\mu \frac{r}{r^3}$$

$$g_x = -\mu \frac{x}{(x^2 + y^2 + z^2)^{3/2}}$$

$$g_y = -\mu \frac{y}{(x^2 + y^2 + z^2)^{3/2}}$$

$$g_z = -\mu \frac{z}{(x^2 + y^2 + z^2)^{3/2}}$$

$$G(\underline{r}) = \begin{bmatrix} \frac{\partial g_x}{\partial x} & \frac{\partial g_x}{\partial y} & \frac{\partial g_x}{\partial z} \\ \frac{\partial g_y}{\partial x} & \frac{\partial g_y}{\partial y} & \frac{\partial g_y}{\partial z} \\ \frac{\partial g_z}{\partial x} & \frac{\partial g_z}{\partial y} & \frac{\partial g_z}{\partial z} \end{bmatrix}$$

$$\frac{\partial g_x}{\partial x} = -\mu \left[\frac{(x^2 + y^2 + z^2)^{3/2} - 3x^2(x^2 + y^2 + z^2)^{1/2}}{(x^2 + y^2 + z^2)^3} \right] = g_{xx}$$

$$\frac{\partial g_x}{\partial y} = \mu \left[\frac{3xy}{(x^2 + y^2 + z^2)^{5/2}} \right] = g_{xy}$$

$$\frac{\partial g_x}{\partial z} = \mu \left[\frac{3xz}{(x^2 + y^2 + z^2)^{5/2}} \right] = g_{xz}$$

$$\frac{\partial g_y}{\partial x} = \mu \left[\frac{3xy}{(x^2 + y^2 + z^2)^{5/2}} \right] = g_{yx}$$

$$\frac{\partial g_y}{\partial y} = -\mu \left[\frac{(x^2 + y^2 + z^2)^{3/2} - 3y^2(x^2 + y^2 + z^2)^{1/2}}{(x^2 + y^2 + z^2)^3} \right] = g_{yy}$$

$$\frac{\partial g_y}{\partial z} = \mu \left[\frac{3xz}{(x^2 + y^2 + z^2)^{5/2}} \right] = g_{yz}$$

$$\frac{\partial g_z}{\partial x} = \mu \left[\frac{3xz}{(x^2 + y^2 + z^2)^{5/2}} \right] = g_{zx}$$

$$\frac{\partial g_z}{\partial y} = \mu \left[\frac{3xz}{(x^2 + y^2 + z^2)^{5/2}} \right] = g_{zy}$$

$$\frac{\partial g_z}{\partial z} = -\mu \left[\frac{(x^2 + y^2 + z^2)^{3/2} - 3z^2(x^2 + y^2 + z^2)^{1/2}}{(x^2 + y^2 + z^2)^3} \right] = g_{zz}$$

Considering the coplanar case, we have $z=0$ and the matrices $G(r)$ and $\dot{G}(r)$.

g_{zz} is not zero but the fact that we work in a coplanar case, we will not consider that term.

$$(6.4) \quad G(\underline{r}) = \begin{bmatrix} g_{xx} & g_{xy} \\ g_{yx} & g_{yy} \end{bmatrix}$$

$$(6.5) \quad \dot{G}(\underline{r}) = \begin{bmatrix} \dot{g}_{xx} & \dot{g}_{xy} \\ \dot{g}_{yx} & \dot{g}_{yy} \end{bmatrix}$$

Let's calculate $\dot{G}(\underline{r})$:

$$\dot{g}_{xx} = -3\mu \left\{ (x\dot{x} + y\dot{y}) \left[5x^2(x^2 + y^2)^{-7/2} - (x^2 + y^2)^{-5/2} \right] - 2x\dot{x}(x^2 + y^2)^{-5/2} \right\}$$

$$\dot{g}_{xy} = 3\mu \left[(\dot{x}y + x\dot{y})(x^2 + y^2)^{-5/2} - 5(x^2\dot{x}y + y^2\dot{y}x)(x^2 + y^2)^{-7/2} \right]$$

$$\dot{g}_{yx} = \dot{g}_{xy} = 3\mu \left[(xy + x\dot{y})(x^2 + y^2)^{-5/2} - 5(x^2\dot{x}y + y^2\dot{y}x)(x^2 + y^2)^{-7/2} \right]$$

$$\dot{g}_{yy} = -3\mu \left\{ (x\dot{x} + y\dot{y}) \left[5y^2(x^2 + y^2)^{-7/2} - (x^2 + y^2)^{-5/2} \right] - 2y\dot{y}(x^2 + y^2)^{-5/2} \right\}$$

Using the equation (6.1) :

$$\underline{r}^{(4)} = \dot{G}(\underline{r})\dot{\underline{r}}(t) + 2G(\underline{r})\ddot{\underline{r}}(t) - G(\underline{r})g(\underline{r})$$

and substituting $\dot{G}(\underline{r})$, $G(\underline{r})$ and $g(\underline{r})$, we obtain :

$$\begin{bmatrix} x^{(4)} \\ y^{(4)} \end{bmatrix} = \begin{bmatrix} \dot{g}_{xx} & \dot{g}_{xy} \\ \dot{g}_{yx} & \dot{g}_{yy} \end{bmatrix} \begin{bmatrix} \dot{x} \\ \dot{y} \end{bmatrix} + 2 \begin{bmatrix} g_{xx} & g_{xy} \\ g_{yx} & g_{yy} \end{bmatrix} \begin{bmatrix} \ddot{x} \\ \ddot{y} \end{bmatrix} - \begin{bmatrix} g_{xx} & g_{xy} \\ g_{yx} & g_{yy} \end{bmatrix} \begin{bmatrix} g_x \\ g_y \end{bmatrix}$$

$$(6.6) \quad \begin{aligned} x^{(4)} - 2g_{xx}\ddot{x} - 2g_{xy}\ddot{y} - \dot{g}_{xx}\dot{x} - \dot{g}_{xy}\dot{y} + g_{xx}g_x + g_{xy}g_y &= 0 \\ y^{(4)} - 2g_{yx}\ddot{x} - 2g_{yy}\ddot{y} - \dot{g}_{yx}\dot{x} - \dot{g}_{yy}\dot{y} + g_{yx}g_x + g_{yy}g_y &= 0 \end{aligned}$$

REFERENCES

- A. Bryson, Applied Optimal Control, Blaisdell Pub. Co, Waltham, Mass, 1969.
- T. E. Carter, "Optimal Power-Limited Rendezvous for Linearized Equations of Motion", AIAA Journal of Guidance, Control, and Dynamics, Vol.17, No.5, September-October 1994, pp 1082-1086.
- T. E. Carter and J. Brient, "Fuel-Optimal Rendezvous for Linearized Equations of Motion", AIAA Journal of Guidance, Control, and Dynamics, Vol.15, No.6, Novembre-December 1992, pp 1411-1416.
- J. H. Chiu, "Optimal Multiple-Impulse Nonlinear Orbital Rendezvous", MSc Thesis, University of Illinois at Urbana-Champaign, 1984.
- G. Colasurdo and D. Pastrone, "An Indirect Method For Fixed-Time Finite-Thrust Optimal Orbit Transfer", AAS paper 93-146.
- V. Coverstone-Carroll, "Optimal Cooperative Power-Limited Rendezvous", Ph.D. Thesis, University of Illinois at Urbana-Champaign, 1992.
- V. Coverstone-Carroll and J. E. Prussing, "Optimal Cooperative Power-Limited Rendezvous Between Neighboring Circular Orbits", AIAA Journal of Guidance, Control, and Dynamics, Vol.16, No.6, November-December 1993, pp 1045-1054.
- V. Coverstone-Carroll and J. E. Prussing, "Optimal Cooperative Power-Limited Rendezvous Between Coplanar Circular Orbits", AIAA Journal of Guidance, Control, and Dynamics, Vol.17, No.5, September-October 1994, pp 1096-1102.
- E. A. Euler, Optimal Low-Thrust Rendezvous Control, AIAA Journal of Guidance, Control, and Dynamics, Vol.7, No.6, June 1969, pp 1140-1144.

- C. R. Hargraves and S. W. Paris, "Direct Trajectory Optimization Using Nonlinear Programming and Collocation", *AIAA Journal of Guidance, Control, and Dynamics*, Vol.10, No.4, July-August 1987, pp 338-342.
- M. Humi, "Fuel-Optimal Rendezvous in a General Central Force Field", *AIAA Journal of Guidance, Control, and Dynamics*, Vol.16, No.1, January-February 1993, pp 215-219.
- C. A. Larson and J. E. Prussing, "Optimal Orbital Rendezvous Using High and Low Thrust", AAS paper 89-354.
- D. F. Lawden, *Optimal Trajectories for Space Navigation*, Butterworths, London, 1963.
- C. A. Lembeck and J.E. Prussing, "Optimal Impulsive Intercept with Low-Thrust Rendezvous Return", *AIAA Journal of Guidance, Control, and Dynamics*, Vol.16, No.3, May-June 1993, pp 426-433.
- K. Mirfakhraie and B.A. Conway, "Optimal Cooperative Time-Fixed Impulsive Rendezvous", AIAA Paper 90-2962, AIAA/AAS Astrodynamics Conference, August 1990, Portland, OR.
- K. Mirfakhraie, "Optimal Cooperative Time fixed Impulsive Rendezvous", Ph.D. Thesis, University of Illinois at Urbana-Champaign, 1991.
- S. P. Murphy, "A Study of Optimal Power-Limited Spacecraft Trajectories", MSc Thesis, University of Illinois at Urbana-Champaign, 1992.
- C. J. Pardis and T. E. Carter, "Optimal Power-Limited Rendezvous with Thrust Saturation", *AIAA Journal of Guidance, Control, and Dynamics*, Vol.18, No.5, September-October 1995, pp 1145-1150.
- J. E. Prussing and J. H. Chiu, "Optimal Multiple-Impulse Time-Fixed Rendezvous Between Circular Orbits", *AIAA Journal of Guidance, Control, and Dynamics*, Vol.9, No.1, January-February 1986, pp 17-22.
- J. E. Prussing (a), "Equation for Optimal Power - Limited Spacecraft

- Trajectories", AIAA Journal of Guidance, Control, and Dynamics, Vol.16, No.2, March-April 1993, pp 391-393.
- J. E. Prussing (b), "Equation for Optimal Power-Limited Spacecraft Trajectories", AAS paper 93-147.
- J. E. Prussing and B. A. Conway (c), Orbital Mechanics, Oxford University Press, NY, 1993.
- J.E. Prussing and B.A. Conway, "Optimal Terminal Maneuver for Cooperative Impulsive Rendezvous", AIAA Journal of Guidance, Control, and Dynamics, Vol.12, May-June 1989, pp 433-435.
- J. E. Prussing and R. S. Clifton, "Optimal Multiple-impulse Satellite Evasive Maneuvers", AIAA Journal of Guidance, Control, and Dynamics, Vol.17, No.3, May-June 1994, pp 599-606 .
- W. A. Scheel and B. A. Conway, "Optimization of Very-Low-Thrust, Many-Revolutions Spacecraft trajectories", AIAA Journal of Guidance, Control, and Dynamics, Vol.17, No.6, November-December 1994, pp 1185-1192.
- P. V. Subba Rao and R. V. Ramanan, "Optimum Rendezvous Transfer Between Coplanar Heliocentric Elliptic Orbits Using Solar Sail", AIAA Journal of Guidance, Control, and Dynamics, Vol.15, No.6, November-December 1992, pp 1507-1509.
- S. Tang and B. A. Conway, "Optimization of Low-Thrust Interplanetary Trajectories Using Collocation and Nonlinear Programming", AIAA Journal of Guidance, Control, and Dynamics, Vol.18, No.3, May-June 1995, pp 599-604.
- J. Tschauner, Elliptic Orbit Rendezvous, AIAA Journal of Guidance, Control, and Dynamics, Vol.5, No.6, November-December 1967, pp 1110-1113.
- L. J. Wellnitz and J.E. Prussing, "Optimal Trajectories for Time-Constrained Rendezvous Between Arbitrary Conic Orbits", AAS paper 87-539.
- D. Zwillinger, Handbook of Differential Equations, Academic Presse, NY, 1989.